Potential of VIIRS Time Series Data for Aiding the USDA Forest Service Early Warning System for Forest Health Threats: A Gypsy Moth Defoliation Case Study

Joseph P. Spruce[1], Robert E. Ryan[1], James Smoot[1], Phillip Kuper[1], Donald Prados[2], Jeffrey Russell[2], Kenton Ross[1], Gerald Gasser[3], Steven Sader[4], Rodney McKellip[5]

[1]Science Systems and Applications, Inc.,
John C. Stennis Space Center, Mississippi

[2]Computer Sciences Corporation,
John C. Stennis Space Center, Mississippi

[3]Lockheed Martin Mission Services – Civil Programs,
John C. Stennis Space Center, Mississippi

[4]University of Maine,
Orono, Maine

[5]National Aeronautics and Space Administration,
John C. Stennis Space Center, Mississippi

National Aeronautics and
Space Administration

John C. Stennis Space Center
SSC, Mississippi 39529–6000

September 20, 2007

Potential of VIIRS Time Series Data for Aiding the USDA Forest Service Early Warning System for Forest Health Threats: A Gypsy Moth Defoliation Case Study

Acknowledgments

Participation in this work by Science Systems and Applications, Inc., and by Computer Sciences Corporation was supported by NASA at the John C. Stennis Space Center, Mississippi, under Task Order NNS04AB54T.

The authors appreciate the contributions of Roxzana Moore, Mary Pagnutti, Slawek Blonski, and Marcia Wise, Science Systems and Applications, Inc., and of Ronald Vaughan, Computer Sciences Corporation, to the preparation of this report. Ted Mason and Craig Peterson of the National Aeronautics and Space Administration provided timely guidance and assistance in the undertaking of this work.

Table of Contents

Tables

Figures

This page intentionally blank

Executive Summary

This report details one of three experiments performed during FY 2007 for the NASA RPC (Rapid Prototyping Capability) at Stennis Space Center. This RPC experiment assesses the potential of VIIRS (Visible/Infrared Imager/Radiometer Suite) and MODIS (Moderate Resolution Imaging Spectroradiometer) data for detecting and monitoring forest defoliation from the non-native Eurasian gypsy moth (*Lymantria dispar*). The intent of the RPC experiment was to assess the degree to which VIIRS data can provide forest disturbance monitoring information as an input to a forest threat EWS (Early Warning System) as compared to the level of information that can be obtained from MODIS data.

The USDA Forest Service (USFS) plans to use MODIS products for generating broad-scaled, regional monitoring products as input to an EWS for forest health threat assessment. NASA SSC is helping the USFS to evaluate and integrate currently available satellite remote sensing technologies and data products for the EWS, including the use of MODIS products for regional monitoring of forest disturbance.

Gypsy moth defoliation of the mid-Appalachian highland region was selected as a case study. Gypsy moth is one of eight major forest insect threats listed in the Healthy Forest Restoration Act (HFRA) of 2003; the gypsy moth threatens eastern U.S. hardwood forests, which are also a concern highlighted in the HFRA of 2003. This region was selected for the project because extensive gypsy moth defoliation occurred there over multiple years during the MODIS operational period. This RPC experiment is relevant to several nationally important mapping applications, including agricultural efficiency, coastal management, ecological forecasting, disaster management, and carbon management.

In this experiment, MODIS data and VIIRS data simulated from MODIS were assessed for their ability to contribute broad, regional geospatial information on gypsy moth defoliation. Landsat and ASTER (Advanced Spaceborne Thermal Emission and Reflection Radiometer) data were used to assess the quality of gypsy moth defoliation mapping products derived from MODIS data and from simulated VIIRS data. The project focused on use of data from MODIS Terra as opposed to MODIS Aqua mainly because only MODIS Terra data was collected during 2000 and 2001—years with comparatively high amounts of gypsy moth defoliation within the study area.

The project assessed the quality of VIIRS data simulation products. Hyperion data was employed to assess the quality of MODIS-based VIIRS simulation datasets using image correlation analysis techniques. The ART (Application Research Toolbox) software was used for data simulation. Correlation analysis between MODIS-simulated VIIRS data and Hyperion-simulated VIIRS data for red, NIR (near-infrared), and NDVI (Normalized Difference Vegetation Index) image data products collectively indicate that useful, effective VIIRS simulations can be produced using Hyperion and MODIS data sources. The r^2 for red, NIR, and NDVI products were 0.56, 0.63, and 0.62, respectively, indicating a moderately high correlation between the 2 data sources. Temporal decorrelation from different data acquisition times and image misregistration may have lowered correlation results.

The RPC experiment also generated MODIS-based time series data products using the TSPT (Time Series Product Tool) software. Time series of simulated VIIRS NDVI products were produced at approximately 400-meter resolution GSD (Ground Sampling Distance) at nadir for comparison to MODIS NDVI products at either 250- or 500-meter GSD. The project also computed MODIS (MOD02) NDMI (Normalized Difference Moisture Index) products at 500-meter GSD for comparison to NDVI-based products. For each year during 2000–2006, MODIS and VIIRS (simulated from MOD02) time series were computed during the peak gypsy moth defoliation time frame in the study area (~June 10 through July 27).

Gypsy moth defoliation mapping products from simulated VIIRS and MOD02 time series were produced using multiple methods, including image classification and change detection via image differencing. The latter enabled an automated defoliation detection product computed using percent change in maximum NDVI for a peak defoliation period during 2001 compared to maximum NDVI across the entire 2000–2006 time frame. Final gypsy moth defoliation mapping products were assessed for accuracy using randomly sampled locations found on available geospatial reference data (Landsat and ASTER data in conjunction with defoliation map data from the USFS).

Extensive gypsy moth defoliation patches were evident on screen displays of multitemporal color composites derived from MODIS data and from simulated VIIRS vegetation index data. Such defoliation was particularly evident for 2001, although widespread denuded forests were also seen for 2000 and 2003. These visualizations were validated using aforementioned reference data. Defoliation patches were visible on displays of MODIS-based NDVI and NDMI data. The viewing of apparent defoliation patches on all of these products necessitated adoption of a specialized temporal data processing method (e.g., maximum NDVI during the peak defoliation time frame). The frequency of cloud cover necessitated this approach.

Multitemporal simulated VIIRS and MODIS Terra data both produced effective general classifications of defoliated forest versus other land cover. For 2001, the MOD02-simulated VIIRS 400-meter NDVI classification produced a similar yet slightly lower overall accuracy (87.28 percent with 0.72 Kappa) than the MOD02 250-meter NDVI classification (88.44 percent with 0.75 Kappa). The MOD13 250-meter NDVI classification had a lower overall accuracy (79.13 percent) and a much lower Kappa (0.46). The report discusses accuracy assessment results in much more detail, comparing overall classification and individual class accuracy statistics for simulated VIIRS 400-meter NDVI, MOD02 250-meter NDVI, MOD02-500 meter NDVI, MOD13 250-meter NDVI, and MOD02 500-meter NDMI classifications.

Automated defoliation detection products from simulated VIIRS and MOD02 data for 2001 also yielded similar, relatively high overall classification accuracy (85.55 percent for the VIIRS 400-meter NDVI versus 87.28 percent for the MOD02 250-meter NDVI). In contrast, the USFS aerial sketch map of gypsy moth defoliation showed a lower overall classification accuracy at 73.64 percent. The overall classification Kappa values were also similar for the VIIRS (~0.67 Kappa) versus the MOD02 (~0.72 Kappa) automated defoliation detection product, which were much higher than the values exhibited by the USFS sketch map product (overall Kappa of ~0.47). The report provides additional details on the accuracy of automated gypsy moth defoliation detection products compared with USFS sketch maps.

The results suggest that VIIRS data can be effectively simulated from MODIS data and that VIIRS data will produce gypsy moth defoliation mapping products that are similar to MODIS-based products. The results of the RPC experiment indicate that VIIRS and MODIS data products have good potential for integration into the forest threat EWS.

The accuracy assessment was performed only for 2001 because of time constraints and a relative scarcity of cloud-free Landsat and ASTER data for the peak defoliation period of the other years in the 2000–2006 time series. Additional work should be performed to assess the accuracy of gypsy moth defoliation detection products for additional years.

The study area (mid-Appalachian highlands) and application (gypsy moth forest defoliation) are not necessarily representative of all forested regions and of all forest threat disturbance agents. Additional work should be performed on other inland and coastal regions as well as for other major forest threats. More work on gypsy moth defoliation detection should also be initiated with other atmospherically corrected MODIS and simulated VIIRS data products. In addition to NDVI, other detection techniques (e.g., NDMI) should be evaluated more thoroughly.

Joseph P. Spruce, Robert E. Ryan, James Smoot, Phillip Kuper, Kenton Ross, Donald Prados, Jeffrey Russell, Gerald Gasser, Steven Sader, Rodney McKellip

1.0 Introduction

This report describes an RPC (Rapid Prototyping Capability) experiment to assess the potential of VIIRS (Visible/Infrared Imager/Radiometer Suite) time series data for aiding the USDA Forest Service EWS (Early Warning System) for forest health threat assessments. This RPC experiment is relevant to several nationally important mapping applications, including agricultural efficiency, coastal management, ecological forecasting, disaster management, and carbon management.

The Healthy Forests Restoration Act (HFRA) of 2003 mandates to the Secretary of Agriculture that a national EWS be developed for early detection, monitoring, and mitigation of forest health threats (Bosworth, 2006). Many forest health threats pertain to specific inland as well as coastal regions. Implementation of the HFRA is important to coastal management because it can help to mitigate the threat posed by disturbed, degraded forests to coastal water quality (Committee on Ocean Policy, 2007).

In response to the HFRA, the USDA Forest Service (hereafter USFS) has established Eastern and Western Regional Threat Assessment Centers. These forest threat centers have been tasked to develop the EWS, which will include integrated geospatial data to characterize and track forest environmental threats at multiple scales (USFS, 2004a; 2005). In particular, this EWS will consider threats from forest damaging insect and diseases, both exotic and native. Native detrimental insects and diseases collectively damage almost 45 times more total acreage of forest than wildfires and cause at least 5 times more economic impact (Dale et al., 2001). In addition, exotic pests cause annual economic losses in U.S. forest products estimated at 2 billion dollars per year (Pimentel et al., 2000).

The RPC experiment described here assesses the potential of VIIRS and MODIS (Moderate Resolution Imaging Spectroradiometer) data for detecting and monitoring forest defoliation from the non-native Eurasian gypsy moth (*Lymantria dispar*). The USFS is planning to use MODIS products for generating broad-scaled regional monitoring product inputs to the EWS. The RPC experiment compared products from simulated VIIRS data to that from MODIS data. In particular, the experiment generated simulated VIIRS NDVI (Normalized Difference Vegetation Index) products at approximately 400 meters resolution (i.e., Ground Sampling Distance or GSD) at nadir for comparison to MODIS NDVI products at either a 250 or 500 meters GSD. The project also generated MODIS (MOD02)[1] NDMI (Normalized Difference Moisture Index) products at 500 meters GSD for comparison to NDVI-based defoliation detection products. Final gypsy moth defoliation mapping products were assessed for accuracy using randomly sampled locations found on Landsat and ASTER (Advanced Spaceborne Thermal Emission and Reflection Radiometer) data displays in conjunction with available geospatial reference data from the USFS.

As part of the NASA's Applied Sciences Program, the RPC initiative provides a framework to perform RPC data application experiments pertinent to mapping applications of national concern. Such experiments employ research results from current and future NASA-funded Earth-observation missions. The RPC provides accelerated simulation, demonstration, and testing of candidate system configurations. RPC experiments are intended to design and test an informational delivery system employing NASA data and/or modeling contributions for potential input into a partnering agency's decision support tool. Such experiments use NASA Earth science research results and any other supportive elements to test a proposed system's feasibility and value. RPC experiment outcomes, both for or against a particular system configuration, are important in helping NASA define which specific directions and strategies to pursue within the Applied Sciences Program.

[1] MODIS products are described in Appendix B.

2.0 Overview of the USDA Forest Service Early Warning System for Forest Environmental Threats

In recent years, there have been several national and international efforts to build EWSs that require broad regional monitoring of forest and other dominant vegetation conditions. Efforts in the United States include regional- to national-scaled EWSs for forest wildfires (Quayle et al., 2003), droughts (Lin et al., 2006), invasive plant species (FICMNEW, 2003), volcanoes (USGS, 2005), tsunamis (Morrissey, 2006), and forest health (USFS, 2004b). A typical EWS includes the following: 1) risk knowledge; 2) monitoring and warning services; 3) dissemination and communication services; and 4) response capability (United Nations, 2006).

Title VI of the HFRA of 2003 (P.L. 108-148) mandated the development of a comprehensive EWS for potential catastrophic environmental threats to forests (U.S. House, 2003). The USFS and the Bureau of Land Management (2004) have published a report that provides guidelines on implementation of the HFRA. The USFS (2004b) reported on the status of the EWS for forest insect and disease threats. This report describes the EWS as a component model with a conceptual framework and integrated core resources for addressing threats from insects and diseases. In doing so, this EWS employs multiple decisions support tools, largely driven by a need to encourage forest sustainability and to counter the increased threat from damaging insects and diseases. This report discusses four main components of the EWS: 1) identification of potential threats; 2) detection of actual threats; 3) assessment of threat impacts; and 4) response to potential and actual threats (USFS, 2004b). Figure 1 depicts the overall framework of the EWS, including the main components.

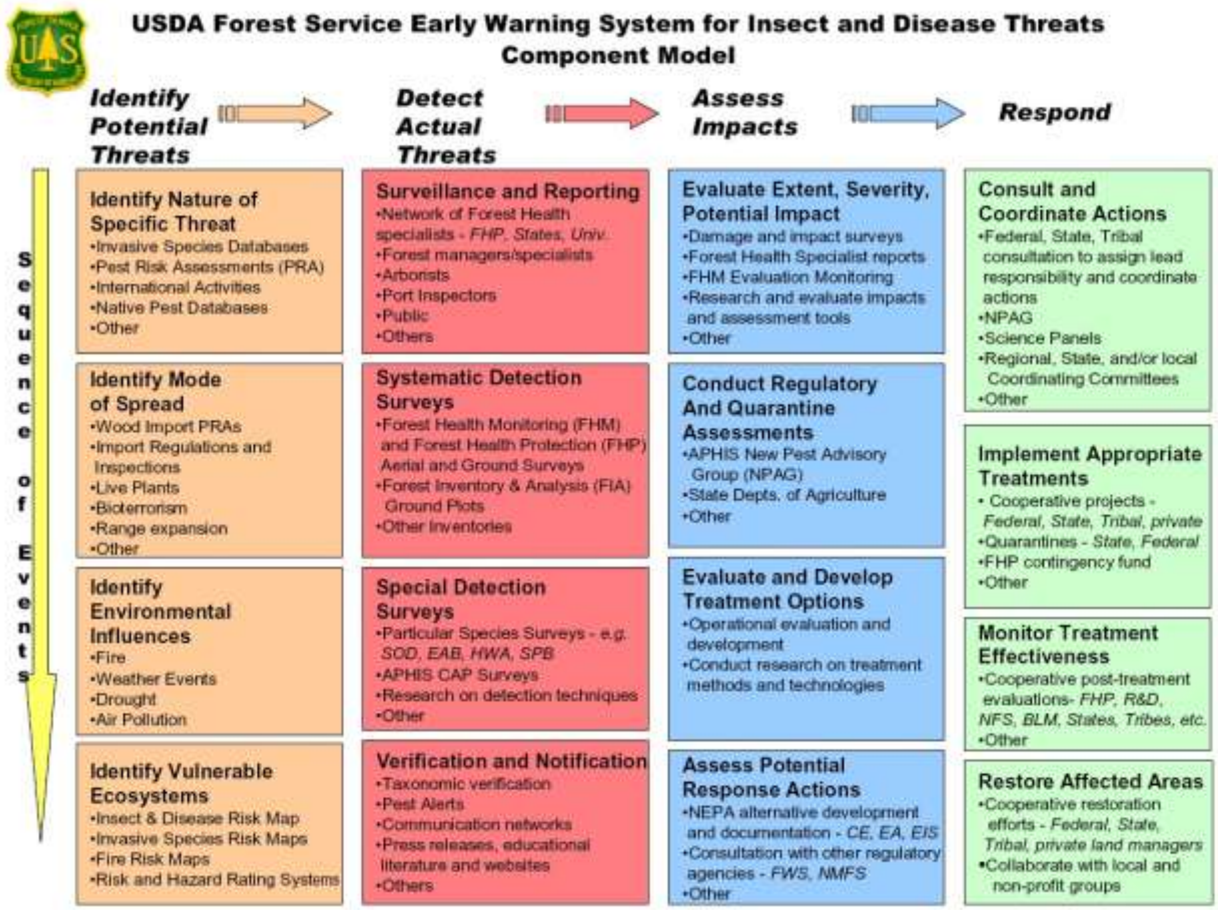

Source: USFS, 2004b

Figure 1. USDA Forest Service Early Warning System for Insect and Disease Threats Component Model.

The USFS has also been working to integrate information from the four components into a computer-aided, Internet-based decision support system. Once the components are sufficiently developed, the system will provide regional to country-wide monitoring and early warning capability in near real time via the Internet. It will yield decision support information on location and extent of a wide range of specific environmental threats, such as damaging invasive species, insects, diseases, hurricanes, drought, wildfire, and land use conversion.

Bosworth (2006) discusses the progress of the EWS since 2004. To aid HFRA Title VI implementation, the USFS established eastern and western U.S. centers for forest environmental threat assessment (Bosworth 2006). Each threat center has regional responsibility and both have collective national responsibility for developing needed infrastructure and capabilities to establish and maintain an EWS for forest health threats. Initial activities are underway to develop, refine, and implement remote-sensing-based forest health anomaly detection capabilities, comparable to what has been done with other Federal Agency EWSs for drought and fire detection and monitoring. In developing the needed applied technologies and infrastructure, the USFS forest threat centers will be integrating remotely sensed data products into the EWS (USFS, 2004a; 2005). NASA SSC is helping the USFS threat centers to evaluate and integrate satellite remote sensing technologies and data products into the EWS (Bosworth, 2006). Remote sensing and expert system technologies are also recommended by Chornesky et al. (2005) as means for improving management of forest threats from invasive species.

Once completed, the EWS will be a multi-scale GIS (Geographic Information System)-based observatory of forest environmental conditions within the United States. The EWS will include continental, regional, and site-specific scales of observations on forest conditions and threats. The USFS intends to use moderate-resolution multitemporal satellite data, such as MODIS and related follow-on data, for the broadest scales of basic forest health monitoring. High-resolution satellite data from Landsat or comparable systems will be used for regional forest assessments, and very high resolution commercial aerial and satellite imagery will be used for more site-specific applications. The EWS will also use FIA (Forest Inventory Assessment) forest health conditions data products derived in part from field surveys.

Aerial sketch mapping of forest defoliation and mortality events is an important facet of the current forest threat monitoring EWS capability. As the plane flies over an area of interest, an analyst interactively screen digitizes outlines of detected forest change polygons onto GPS (Global Positioning System-synchronized GIS map displays of over-flown areas (Schrader-Patton, 2003). Such sketch maps are often used to aid resource managers in performing subsequent forest health management efforts, such as field validation and evaluation surveys. However, aerial sketch maps of forest defoliation and mortality tend to give only a general indication of location, frequently overestimating extent of change within a delineated polygon (Hall et al., 2006). Such sketch maps can also omit detection of defoliation areas. The aerial sketch mapping process involves subjective delineation of defoliation areas, the quality of which depends in part on the experience and skill of the sketch mapping specialist (Ciesla, 2000). The USFS (2007) reports that sketch maps of gypsy moth defoliation can identify areas with 30 percent or more defoliation and can indicate 2 classes of defoliation intensity: medium (30–50 percent) and high (>50 percent). Sketch maps have map georeferencing problems as well (Ciesla, 2000; USFS. 2007). Variable weather conditions can also reduce effectiveness of this technique (Ciesla, 2000; Hall et al., 2006).

The USFS currently performs national forest health threat detection and monitoring surveys using a nationally standardized aerial and ground survey approach to evaluate status and change in forest conditions (Ellenwood, 2006). The USFS National Forest Health Monitoring Program is assessing and working toward a future, multi-tiered approach to forest health monitoring, including the following: 1) Tier 0 - vulnerability assessment; 2) Tier 1 - synoptic surveillance; 3) Tier 2 - focused surveillance; 4) Tier 3 - directed monitoring (for validation of Tier 1 and 2 products); and 5) Tier 4 - project assessment (for site-specific needs) (Ellenwood, 2006). The USFS has also been developing and assessing regional disturbance mapping products from MODIS data, though these products are still experimental (Ellenwood, 2006; Nielson et al., 2006).

Forest threat assessment involves an integrated combination of detection, monitoring, assessment, and mitigation capabilities that have been greatly augmented in recent years by new geospatial data sources and analytical GIS technologies. Great advances have been made in the development of predictive geospatial models depicting risk of damage and mortality due to specific pests (e.g., Morin et al., 2004). Such models will play a crucial role in the development of a forest threat EWS by enabling analysts to compare detected forest health anomalies to areas having high risk of damage from a specific pest, such as the Eurasian Gypsy Moth.

The USFS is working to implement a forest threat EWS, although details on the actual architecture are still emerging. The USFS Eastern Forest Threat Center is developing a system known as the FIRST (Forest Incidence Recognition and State Tracking System), described by Hargrove and Hoffman (2006). The FIRST will eventually employ multitemporal MODIS data as input, tentatively using Collection 5 MOD43B4 data bundled as 16-day composites. As of this writing, the Collection 5 was not available for the entire United States over the MODIS operational period. The MOD43B4 data will include 500 m MODIS Nadir Bidirectional Reflectance Distribution Function Adjusted Reflectance bands, although this resolution of data is only partially available as of this writing. The FIRST will employ multivariate analysis of geospatial data on forest vegetation, climate, soils, and topography to detect and track forest threats. Other EWS architectural design elements have been also been presented by Nielsen and Finco (2006) and Ryan (2006), although there is significant commonality among these designs, including that MODIS data will be a critical input to the system. Other MODIS data products and processing strategies are currently being assessed by the USFS and NASA SSC in an effort to reach a final determination on which MODIS product(s) would best meet the requirements of the operational EWS.

3.0 Historic Use of MODIS Data in Regards to Forest Threat Assessment and EWS Applications

3.1 Previous Use of MODIS Data for Addressing Monitoring Needs of the Forest Threat EWS

The EWS for forest threats will need to include a broad regional forest monitoring capability in which forest disturbance can be identified and assessed according to causal agent. A variety of disturbance agents threaten forests in the United States and globally, including native insects and disease, exotic insects and disease, invasive plants, drought, wildfire, hurricanes, tornados, and ice storms. Forest management practices, land use change, air pollution, land subsidence, salt water intrusion, and climate change can also pose threats to forests.

After the fact, forest disturbance monitoring with remote sensing has been demonstrated using moderate-resolution data, although its success may depend upon disturbance patch characteristics and the availability of cloud-free data. In hindcast mode, remote sensing Earth scientists have shown that forest disturbance can be mapped if the event occurred across areas greater or equal to a single pixel spatial resolution. One pixel at the highest resolution of MODIS (250 m) corresponds to an area of 6.25 ha or 15.44 acres.

Moderate-resolution satellite data has also been used to monitor insect-induced forest disturbance. In particular, multitemporal data from AVHRR (Advanced Very High Resolution Radiometer), SPOT (Système Probatoire d'Observation de la Terre) VEGETATION, and MODIS have been used to detect broad regional insect-induced forest damage. Breshears et al. (2005) applied multitemporal (AVHRR) NDVI to detect and assess bark-beetle-induced mortality of pinyon pine juniper forest in the southwestern United States. Ranson et al. (2006) used multitemporal MODIS and SPOT VEGETATION data to detect Siberian silk moth damage to taiga forests in Siberia, reporting a ≥90 percent outbreak detection accuracy for both data sources. Kharuk et al. (2004) employed AVHRR to detect Siberian silk moth outbreaks in eastern Siberia, mapping 2 classes of damage intensity in terms of heavy (50–75 percent mortality) and very heavy (≥75 percent mortality). Potter et al. (2005) reported that global AVHRR data products resampled to 8-km pixels were able to detect extensive forest insect outbreaks. Ramsey et al. (2001) used multitemporal AVHRR and single-date Landsat data to assess extent of hurricane damage to coastal Louisiana forest cover types, including defoliation of deciduous coniferous and broad-leaved forest types.

Jin and Sader (2005a) studied the effect of forest disturbance patch size on detection accuracy. They found that use of the 16-day composite NDVI data (MOD13QKM) achieved 69 percent detection accuracy and that use of the single day NDVI (MOD02QKM) achieved 76 percent detection accuracy when the disturbed patch size was greater than 20 ha. The detection accuracy increased to approximately 90 percent for both datasets when the patch size exceeded 50 ha. The r^2 (range 0.6 to 0.9) and slope (range 0.5 to 0.9) of regression lines between Landsat and MODIS data (based on forest disturbance percent of township) increased with the mean disturbed patch size of each township.

MODIS has shown an ability to detect broad-scaled forest disturbance, although it is less likely to enable detection from a specific causal agent unless the agent is predominant over others. MODIS and other multitemporal moderate-resolution data have been used to assess specific kinds of forest damage in situations in which the damage has predominantly one causal agent. In cases of multiple concurrent disturbance agents, such satellite data can achieve disturbance detection, but the underlying causal agent cannot be determined. However, the latter can be assessed by integrating additional geospatial data sources (e.g., combined use of FIA and MODIS data to model regional risk of damage due to a specific threat). This multi-data source approach is being used by the USFS in the development of geospatial models for specific forest threat risks (Lewis, 2002; Morin et al., 2005; Krist, 2007; Logan et al., 2007).

Multispectral vegetation indices and transformations have been used extensively in forest change detection studies. The NDVI, perhaps the most well known and popular vegetation index, contrasts the visible red and NIR (near infrared) wavebands, which are available on most multispectral satellite systems. Other indices, including NDMI and TCW (Tasseled Cap Wetness), have been applied with forest change detection results in several studies, equal to or exceeding those using NDVI. Jin and Sader (2005b) indicated that the NDMI and TCW were highly correlated (>0.95 r^2) for all five Landsat image dates in their study. One advantage of NDMI over the TCW is that it can be calculated using any sensor that has 2 bands corresponding to the NIR and SWIR (short-wave infrared) regions of the spectrum.

Recent studies by Hayes and others (e.g., Hayes and Cohen, 2007; Hayes et al., in press) indicated the importance of the SWIR bands on MODIS, and particularly the NDMI, that outperformed other popular vegetation indices tried (including NDVI and tasseled cap greenness and wetness) in detecting and modeling forest disturbances associated with harvesting and clearing. The NDMI was used in these studies for its ease in calculation with MOD02 single-day 500 m data. The NDMI was calculated for the MOD02HKM dataset by contrasting the visible red (MOD02 band 2) and SWIR band (MOD02 band 6).

It is not clear whether NDMI or NDVI would be better in monitoring broad-leaved forest defoliation with MODIS or VIIRS, although it may depend on forest damage symptomatology and cover type. Vogelmann (1990) compared Landsat NDVI and SWIR/NIR ratio imagery on several forest cover types subjected to biotic or abiotic forest damage. He concluded: 1) the SWIR/NIR ratio was superior in identifying low versus high forest damage in areas with balsam fir mortality; 2) both SWIR/NIR and NDVI distinguished between low and high damage on deciduous (broad-leaved) forest sites; and 3) NDVI was superior in separating medium and low damage within deciduous forest.

Multitemporal, moderate-resolution satellite data has been used with varying success to monitoring insect defoliation, depending upon avoidance of cloud cover during the time of peak defoliation and the extensiveness of the defoliation. Many of these application projects are essentially opportunistic research as opposed to operational in nature. The USFS is not yet using MODIS data for operational regional forest health monitoring, although work is being done toward this goal (Ellenwood, 2006; Nielsen et al., 2006). In addition, 250 m MODIS data is now being employed in part to develop forest type maps needed for forest threat risk assessment (Brewer et al., 2005). The USFS has adopted operation of near real time multitemporal MODIS data for wildfire detection (Quayle et al., 2003). Recent advances in remote sensing time series data processing has led to a belief that multitemporal MODIS and follow-on VIIRS data has a significant role to play in the forest health monitoring and threat EWS applications.

A growing number of applications use multitemporal MODIS-based NDVI for vegetation anomaly detection, disturbance mapping, and health assessment. Such applications generally use vegetation index products to compare either single dates or temporal composites depicting disturbed or non-disturbed vegetation. Such applications require that input multispectral data be at least scaled in terms of at-sensor radiance or planetary reflectance. Data that is atmospherically corrected and scaled to ground reflectance can offer additional benefits, especially for multiyear comparisons. For example, Hayes et al. (in press) reported that spectral indices based on atmospherically corrected surface reflectance data produced consistent model parameters and accurate forest cover change estimates when modeling over multiple time intervals.

Depending on the phenomenon, broad-area forest disturbance detection can require spatial resolutions of 250 to 500 meters. Coarser 1-km resolution data has been used for detecting very broad extensive disturbance events. Hayes et al. (in press) tested the effect of MODIS grain size (0.25, 0.50, and 1 km) on forest disturbance detection and model prediction. These authors reported than NDMI calculated from half-kilometer MOD02 calibrated radiance datasets generally showed the best relationships in detecting forest disturbance (forest clearing for agriculture) and the lowest model prediction errors at individual study areas and time intervals.

Cloud-free data is also a requirement for monitoring forest disturbance with electro-optical multispectral sensors. Obtaining single dates of cloud-free, area-wide coverage can be difficult. The scarcity of cloud-free data on single dates may be mitigated when temporal composites of cloud-free data encompass the time during which tree damage symptoms are evident.

3.2 Available NASA Data Compared to Information Requirements for the Forest Threat EWS

Several NASA satellite datasets were initially considered for use in the RPC experiment, with MODIS, Hyperion, Landsat, and ASTER data ultimately selected. These datasets were selected because they have been used for forest defoliation assessments or have sufficient spatial and spectral resolution to be appropriate in these applications. MODIS and Hyperion data were selected for simulating VIIRS data band and vegetation index products, such as NDVI. While MODIS data is similar to VIIRS in terms of map extent and band definitions, its spatial resolution differs from VIIRS. On the other hand, Hyperion satellite data has comparable spectral bands and sufficiently high spatial resolution needed to produce the highest quality simulations of VIIRS vegetation indices in forest assessments, such as NDVI and NDMI. The map extent of a typical Hyperion scene is less than that of VIIRS, particularly in the across-track direction. However, it is sufficient for enabling VIIRS simulations and comparisons to VIIRS simulations from other data sources (e.g., MODIS).

The EWS requires a means to identify and track forest defoliation and disturbance at regional to continental scales. MODIS and VIIRS data simulated from MODIS will be assessed for their ability to contribute broad, regional geospatial information on gypsy moth defoliation, where as Landsat and ASTER data will be used to assess the quality of gypsy moth defoliation mapping products derived from MODIS and simulated VIIRS data.

4.0 Experimental Approach

4.1 Selection of Case Study and Study Area for RPC Experiment

The goal of the experiment is to assess the potential of VIIRS data for monitoring forest defoliation, especially among broad-leaved “hardwood” forests. The most extensive hardwood forests in the Nation occur in the eastern United States. The HFRA lists eight major U.S. forest insect threats, including four affecting hardwood forests: 1) gypsy moth; 2) emerald ash borer; 3) red oak borer; and 4) white oak borer. The RPC experiment regards application of simulated VIIRS data for detecting and monitoring areas subject to gypsy moth defoliation. The gypsy moth attacks a wide range of hardwood forest species, especially oak-dominated hardwood forests. The current range of gypsy moth occurrence is in the eastern United States, although it is expanding west and southward.

The mid-Appalachian highland region was selected for the project because of gypsy moth defoliation occurring over multiple years during the MODIS operational period (Figure 2). This area encompasses portions of 4 states (West Virginia, Virginia, Pennsylvania, and Maryland) and a total area of approximately 15 million acres. It is largely forested with eastern hardwood species, including an abundance of oak-dominated forests occurring along an extensive network of ridges. Much of the valleys in this region are in non-forested land use subject to agriculture.

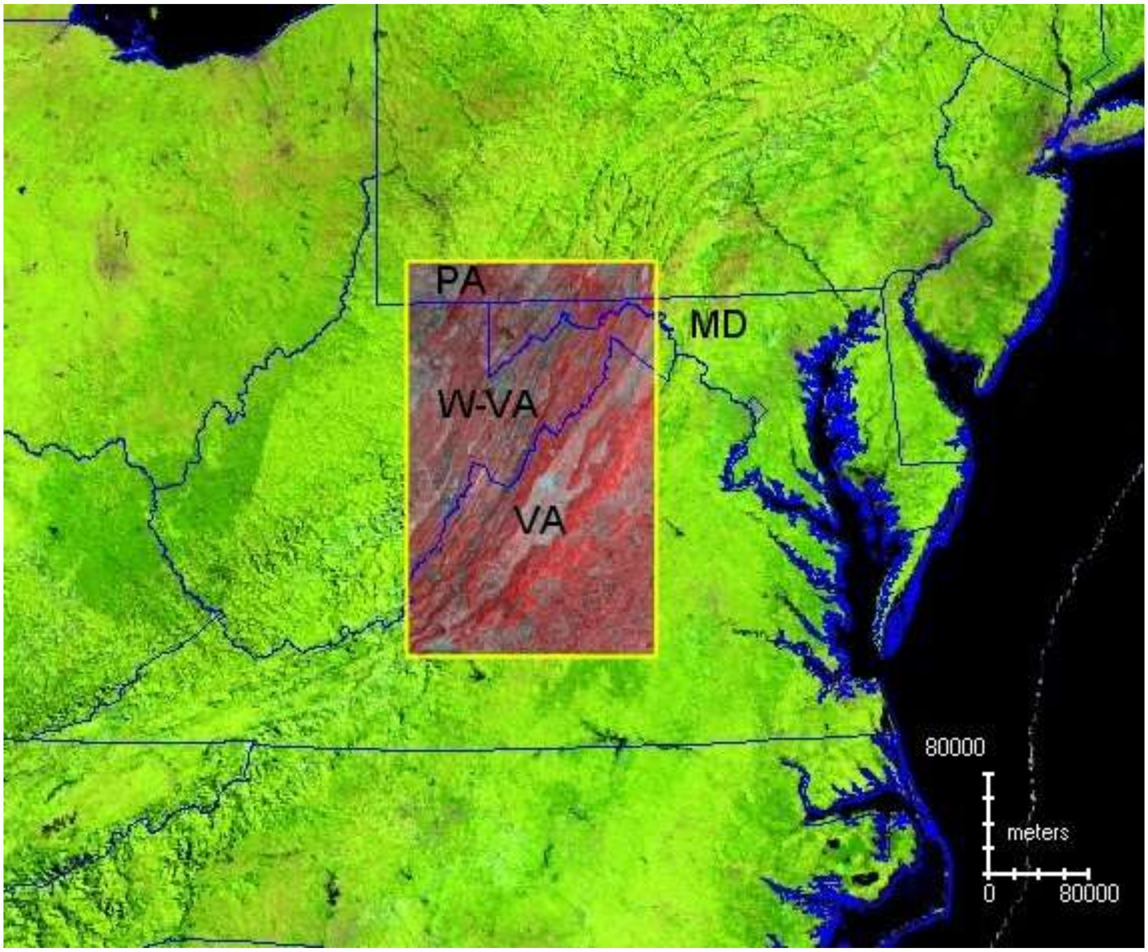

Figure 2. Location of study area in the eastern United States (study area extent indicated in yellow shown with Landsat mosaic in foreground and MODIS mosaic in background).

4.2 Data Acquisition

Much data acquisition and preprocessing occurred before VIIRS simulation. Several MODIS Aqua and Terra multispectral, multitemporal data products were acquired over the study area for all available dates during the 2000 through 2006 time frame. Primary MODIS formats acquired included MOD02, MOD09, MOD12, MOD13, and MOD43 products. MOD03 and MOD35 products were also acquired to mask out cloud-covered and non-useable quality data.

Several high-resolution satellite images from Hyperion, ALI (Advanced Land Imager), Landsat, and ASTER were acquired for use as reference data in the evaluation of VIIRS simulation data products. Figure 3 shows footprints of high-resolution remote sensing data collections in relation to the study area. The two Hyperion scenes were originally acquired on July 24, 2001, and on October 6, 2002, respectively. Several Landsat 5 and 7 scenes were obtained from collections made in the 1999–2006 time frame. Multiple ASTER scenes were also acquired, including two scenes acquired on July 24, 2001, the same date as one of the Hyperion scenes.

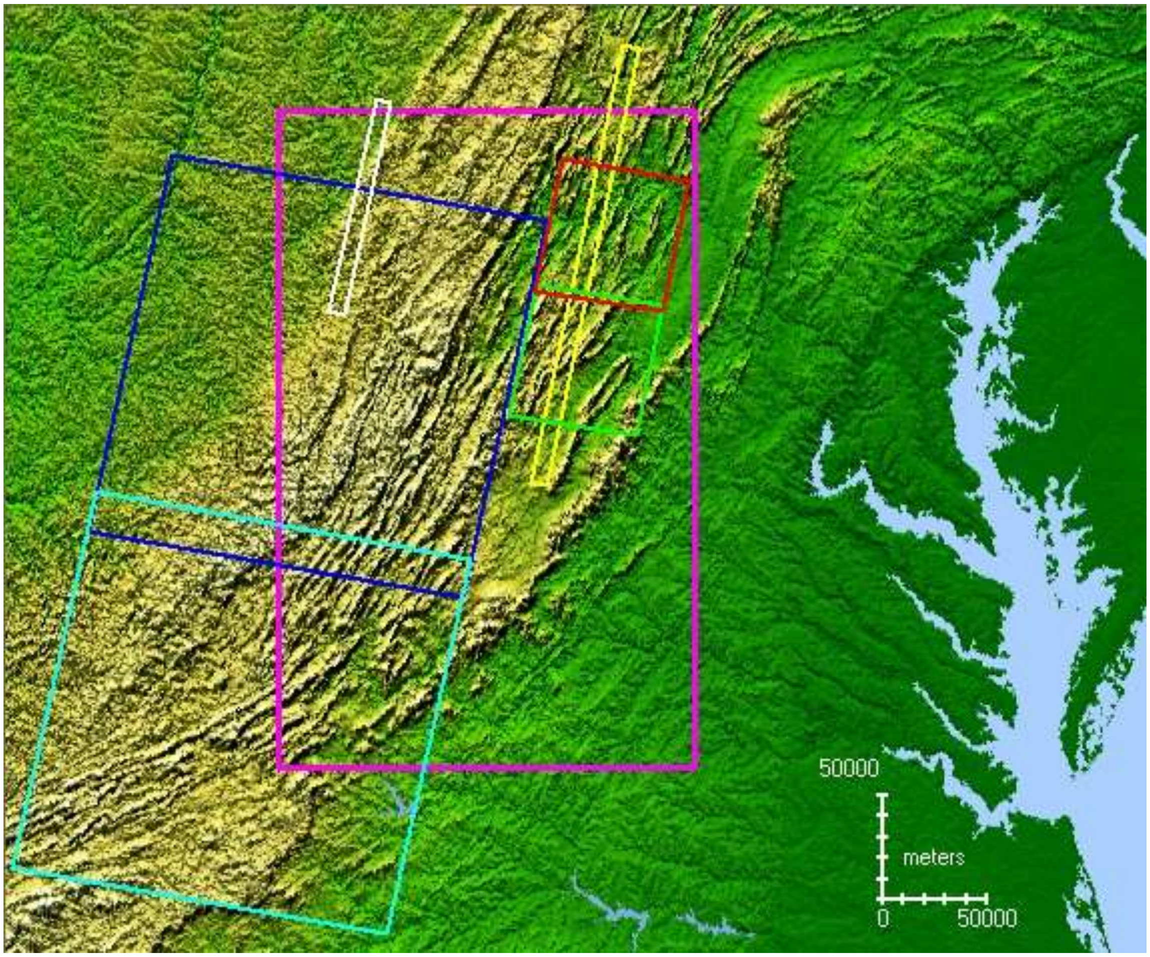

Figure 3. Location of Landsat, ASTER, and Hyperion imagery that was collected over study area (magenta outline) during gypsy moth peak defoliation of 2001. Footprints are overlain on SRTM hill-shaded terrain model with Landsat in blue and cyan, ASTER in red and green, and Hyperion in white and yellow.

4.3 Methods for VIIRS Data Simulation and Validation

4.3.1 Generation of Single-date VIIRS Simulation Datasets

The simulation of VIIRS data was performed using multiple methods and data sources to cross-compare results visually and quantitatively. Hyperion and MODIS data were applied to simulate VIIRS data products for cross comparison, using the ART (Application Research Toolbox) as the main in-house software for data simulation. Blonski et al. (2002), Zanoni et al. (2002), and Ross et al. (2006) describe the development and application of the ART software. Developed in MATLAB®, the ART software enables users to perform a suite of simulations and statistical trade studies on remote sensing systems. In particular, the ART provides the capability to generate simulated multispectral satellite image data at user-specified resolutions using high spatial hyperspectral and/or multispectral satellite image products. For this project, the ART was used to generate simulated VIIRS time series from MOD02 time series.

The basic process used to transform MODIS data into simulated VIIRS data involved the following sequence: 1) swath-oriented radiance data from MODIS was input as HDF file into ART; 2) a blur transformation was variably applied to the input data with 0 to 31 degrees scan angle (weighting of blur dependent on scan angle up to 31 degrees); 3) no blur was applied to input data with ≥31 degrees scan angle; and 4) re-projection of data to UTM map projection and GSD of 400 meters, using the MRT Swath (MODIS Swath Reprojection Tool) from the NASA Goddard Space Flight Center.

In general terms, the process for transforming Hyperion data into simulated VIIRS data involved the following steps: 1) georegistration of Hyperion data to orthorectified Landsat imagery using ERDAS IMAGINE® software; and 2) spectral and spatial synthesis of Hyperion to generate VIIRS spectral bands and spatial resolution of 400 meters. For this study, efforts focused on Hyperion data from July 24, 2001, because the October 6, 2001, Hyperion scene did not include all of the necessary NIR bands and therefore was not used for subsequent simulation. In this study, the ART was used to generate simulated VIIRS data for the red and near-infrared bands needed for generating NDVI products.

The ART enables data to be scaled in either at-sensor radiance or planetary reflectance and can also work with atmospherically corrected data when available. It includes a utility in which an image extent mask is generated for subsequent subsetting of comparable MODIS, simulated MODIS, or simulated VIIRS data derived from MODIS data. The ART incorporates sensor-specific PSF (point spread function) synthesis through a LSE (Least Squares Estimation) and pixel degradation, using a MODIS PSF described by Rojas et al. (2002) and a VIIRS PSF discussed by Schueler et al. (2003). Spectral synthesis of VIIRS data from Hyperion uses an LSE between Hyperion bands and a MODIS or VIIRS spectral band. In the process, ART convolves the input MODIS data to the VIIRS PSF in order to produce MODIS-simulated VIIRS data.

4.3.2 Generation of Simulated VIIRS Time Series

After MODIS-based VIIRS data simulation with ART software, analysts used the TSPT (Time Series Product Tool) to generate time series. MODIS and MODIS-based VIIRS simulation time series data was later used to develop gypsy moth defoliation mapping products.

The process for generating MODIS time series involves the following: MODIS Terra MOD02 data files over the entire 2000–2006 time frame were input into the TSPT. Once the data was read in, the TSPT initially called upon the MRT Swath software to re-project the input data to the UTM map projection. Afterwards, the data was applied to produce NDVI from relevant bands, then cloud masked with the MOD35, further masked to exclude sensor zenith angles greater than 47 degrees, and then temporally filtered so that daily data voids from clouds were filled with temporally interpolated values. By default, temporal filtering used a weighted Savitzky-Golay algorithm based on pixel quality and temporal distance from an individual date of data. This algorithm includes parameter settings for 1) temporal frame size; 2) polynomial order; and 3) FWHM (Full Width Half Maximum) in regard to the temporal distance. These settings are somewhat product dependent. For example, the MOD02-based daily product generation uses a temporal frame size of 15, a polynomial order of 1, and a FWHM of 8. This process was first run on MOD02 250-meter data to compute temporally filtered daily NDVI products and then later repeated to produce temporally filtered 500-meter daily NDMI products for the peak defoliation time frame annually during 2000–2006. MODIS-based VIIRS simulations were processed similarly, except that the input data was from ART simulation output that is already georeferenced.

The TSPT produces intermediate files for each of these steps so that the effect of each processing step could be assessed. It also stacks output from each day into a multitemporal data stack for each year and for all years combined. The final filtered output contains planetary reflectance pixels at 250-meter GSD. This output is projected to a UTM map projection (zone 17, datum and spheroid WGS84). Additional information on the TSPT software and its potential for monitoring vegetation is provided by McKellip et al. (2005) and Prados et al. (2006).

4.3.3 Validation of VIIRS Simulation Data

Validation of MODIS-based VIIRS simulation proceeded as follows: Based on work by Ross et al. (2006), a Hyperion scene from July 24, 2001, was used in a reference capacity to evaluate MODIS data as a means for simulating VIIRS data. Hyperion data was selected because of its hyperspectral and comparatively high spatial resolution characteristics. A cloud-free subset of the Hyperion data was selected. A mask of this image was used to subset the corresponding area on the MODIS data. At that point, the Hyperion and MODIS-based VIIRS simulation datasets were from the same day, nearly concurrent in time of day, and pertained to same area on the ground.

Validation of the simulation results involves a two-tiered approach discussed by Ross et al. (2006). In particular, Hyperion is used as reference data for assessing the quality of VIIRS simulation from MODIS data. For each Hyperion scene, MODIS and simulated MODIS from Hyperion data were then compared via statistical correlation analysis. Doing so provides evidence of Hyperion data suitability for simulating MODIS data. Afterwards, correlation analysis was performed between VIIRS simulated from MODIS and VIIRS simulated from Hyperion data.

Such comparisons were performed to quantify MODIS-based VIIRS simulation errors associated with aliasing and to assess whether high quality, MODIS-derived VIIRS data can be effectively simulated for the study area and application of interest.

4.4 Methods for Detecting Gypsy Moth Defoliation from MODIS-Simulated VIIRS Data

For each year during 2000–2006, MODIS and VIIRS (simulated from MOD02) time series were computed when peak gypsy moth defoliation tends to occur in the study area (June 10 through July 27). ERDAS IMAGINE and ENVI software were used to assess MODIS and simulated VIIRS gypsy moth defoliation mapping products.

On a per-pixel basis, the maximum NDVI value was computed for each year’s peak defoliation period and for all 7 years during this same seasonal time frame. A multi-channel data stack was compiled using the 7 individual years of the maximum NDVI during peak defoliation and of the maximum NDVI during peak defoliation for all 7 years combined. The latter in essence records forest NDVI values during non-defoliated states over the peak defoliation time frame.

The aforementioned data stacks were used to assess the potential of the MODIS-simulated VIIRS data for detecting gypsy moth defoliation through 1) visualization of screen displays from simulated multi-date VIIRS data; 2) assessment of forest defoliation maps from simulated VIIRS data and unsupervised classification; and 3) assessment of automated forest defoliation maps from thresholding change detection products.

Image analysts visualized RGB color composite screen displays derived from the stack to qualitatively assess detectability of defoliation. In doing so, analysts compared the maximum NDVI during peak defoliation across all 7 years (i.e., reference data) to that for a year in which defoliation was common. This technique employs additive color theory in regard to multitemporal imagery as discussed by Sader and Winne (1992). Analysts also used this technique to compare two consecutive defoliation years to reference NDVI during non-defoliation.

A second detection product line was generated using unsupervised classification of one date of maximum NDVI during a given year of peak defoliation and of the maximum NDVI during peak defoliation across all 7 years. This technique was demonstrated for 2001 because it included extensive gypsy moth defoliation that was also recorded with cloud-free Landsat and ASTER imagery. Image classifications were produced for MOD02, MOD13, and simulated VIIRS data products using ISODATA unsupervised clustering and 20 cluster classes per dataset. Classification results were initially assessed using Landsat, ASTER, and Hyperion satellite image displays in conjunction with USFS gypsy moth sketch maps and National Land Cover Data 2001 data products. An interim classification was produced by recoding the 20 classes into 3 land cover categories: 1) non-forest; 2) non-defoliated forest; and 3) defoliated forest. For MODIS 250-meter products, homogenous single-class patches in the recoded image were then aggregated (“clumped”) to dissolve small patches of 4 pixels or less into the dominant class of the surrounding area to reduce commission error visibly apparent with small patches. For MODIS 500-meter and VIIRS 400-meter products, homogenous single-class patches in the recoded image were aggregated to dissolve 2 pixels or less into the dominant class of the surrounding area. Final classifications were then computed by recoding interim classification into 2 classes (defoliated forest versus “other”).

A third line of detection products was computed in which the maximum NDVI for each year’s peak defoliation time frame was compared to the maximum NDVI during peak defoliation across the entire 7-year time span, using the following formula:

$$\%\,Change\ in\ Maximum\ NDVI = \frac{(Maximum\ NDVI\ Peak\ Defoliation\ Year\ X) - (Maximum\ NDVI\ Peak\ Defoliation\ All\ Years)}{(Maximum\ NDVI\ Peak\ Defoliation\ All\ Years)} * 100$$

This percent change in maximum NDVI detection product was computed for 2001 using MOD02 and MOD02-based VIIRS simulation data. This detection product was thresholded so that anomalously high drops in NDVI were defined as greater than ~ -4 percent change. For this product to be useful and comparable in quality to the unsupervised classification, a forest mask was applied to limit thresholding to forested areas. The forest mask was derived from the best apparent MOD02 classification (described above) with healthy and defoliated forest combined as one class. Later, additional masking was done to determine appropriate thresholding values for defoliated forest. A thresholding value of -4 or more percent was used to classify all defoliated forest. The resulting binary image of defoliated forest and other was clumped, and then an eliminate routine was applied to dissolve small patches into the majority class value surrounding them. The elimination patch size was 4 pixels for MODIS 250-meter products, 2 pixels for VIIRS 400-meter products, and 2 pixels for MODIS 500-meter products.

4.5 Method for Validating Gypsy Moth Defoliation Detection Products

The accuracy of each 2001 classification and change detection product was assessed using online reference documentation by the USGS-NPS Vegetation Mapping Program (USGS and NPS, 2007). Accuracy of defoliation mapping products was estimated using the following approach:

1) A stratified random sample of pixels was selected using the best apparent MODIS 250-meter classification (MOD02 NDVI) so that each of 3 classes (non-forest, non-defoliated forest, and defoliated forest) were represented by at least 50 random sample locations.

2) Each sample was of a 3x3 pixel area in which all pixels were of the same class.

3) An analyst viewed each randomly sampled location on either a Landsat or ASTER image taken over the area during June 2000 pre-defoliation and 2001 peak defoliation time frames/

4) Based on interpretation of the Landsat or ASTER RGB displays at a fixed high-resolution viewing scale (1:17,500), the analyst categorized each selected sample location as being either non-forest, non-defoliated forest, or defoliated forest.

5) The results of the Landsat/ASTER image interpretation were cross-compared to each classification via an error matrix to compute percent overall accuracy (i.e., agreement) as well as user and producer accuracy on a per-class basis.

6) Kappa statistics were generated to assess overall classification accuracy adjusted for random chance effects. The latter would be used to assess agreement beyond what is possible through random chance.

In interpreting results of map accuracy assessment, producer accuracy is inversely related to omission error, whereas user accuracy is inversely related to commission error. Accuracy assessment was also performed on 2-class classification products depicting defoliated forest versus “other.” The “other” category was derived by recoding the interim 3-class classifications, combining non-defoliated forest and non-forest categories yet retaining the defoliated forest class.

5.0 Results and Discussion

5.1 Comparison of VIIRS Data Simulations from MODIS and Hyperion Data

MODIS data does not satisfy the Nyquist criterion of being twice the spatial sampling frequency (i.e., GSD) of VIIRS to properly simulate VIIRS from a spatial resolution standpoint most realistically. However, Hyperion data does satisfy the Nyquist criterion both for MODIS simulation and for VIIRS simulation, albeit for a limited spatial extent in the across-track direction. MODIS data provides a better simulation of VIIRS data from a map-extent perspective and is probably sufficiently spatially resolute to approximately simulate VIIRS NDVI products for many test-case scenarios, although the suitability needs to be tested for each application.

In this study, Hyperion-based simulation was used as a reference for validating the ability of MODIS data to simulate VIIRS bands needed for NDVI product generation. Table 1 summarizes the results of comparing Hyperion-simulated MODIS data to actual MODIS data acquired on the same date (July 24, 2001). These comparisons yielded high correlations (r^2 of 0.832 or higher) for the red, NIR, and NDVI image products. The correlations probably were lowered somewhat by the difference in data acquisition times and corresponding differences in atmospheric contaminants (e.g., clouds) on the source MODIS and Hyperion data. The clouds and cloud shadows were mitigated through masking on both the source MODIS and Hyperion data. Bidirectional reflectance and sun glint on water effects may have also caused some lower correlation. Nonetheless, the high correlation provides evidence that Hyperion data is quite capable of simulating MODIS data.

Table 1. Results of correlation analysis: Hyperion-simulated MODIS data versus MODIS data acquired over study area on July 24, 2001.

Comparison	RED r^2	Red RMSE	NIR r^2	NIR RMSE	NDVI r^2	NDVI RMSE
Hyperion-simulated MODIS versus MODIS	0.832	0.005	0.881	0.015	0.877	0.023

Table 2 summarizes the results of correlation analysis between MODIS-simulated VIIRS data and Hyperion-simulated VIIRS data for red, NIR, and NDVI image data products.

Table 2. Results of correlation analysis: MODIS-simulated VIIRS data versus Hyperion-simulated VIIRS data acquired over study area on July 24, 2001.

Comparison	RED r^2	Red RMSE	NIR r^2	NIR RMSE	NDVI r^2	NDVI RMSE
MODIS-simulated VIIRS versus Hyperion-simulated VIIRS	0.561	0.007	0.63	0.024	0.615	0.035

The results of these correlation analyses collectively indicate that useful, effective VIIRS simulations can be produced using Hyperion and MODIS data sources (Table 2). The r^2 for red, NIR, and NDVI products were 0.561 or higher. These results show moderately high correlations that probably are higher in reality due to suspected misregistration between the MODIS and Hyperion datasets. Work by Ross et al. (2006) involved similar comparisons on a more heterogeneous suburban landscape near Kenner, Louisiana, that showed higher correlations ($r^2 \geq 0.71$) for the same three products (red, NIR, and NDVI). The latter study included a dataset co-registration process that has not been performed for this RPC experiment, although the analysis will be run again once the co-registration of the MODIS and Hyperion data is completed. Nonetheless, these studies indicate the value of Hyperion data for understanding the performance of MODIS data in simulating VIIRS red, NIR, and NDVI image products as potential inputs to the forest threat EWS.

The analysis could have benefited from collecting Hyperion data over the study area during peak gypsy moth defoliation. A search for available data indicated two quality scenes. Unfortunately, both datasets were collected after the true peak defoliation period because refoliation was evident. In each case, especially with the September image, ample indication of refoliation showed on the native 30-meter Hyperion data. The Hyperion data used in the VIIRS simulations showed a mixture of defoliated, re-foliated, and never defoliated hardwood forest vegetation. On the upside, these selected subsets were largely cloud free and indicative of common landscape conditions in the study area during the seasons of data collection (mid summer for 2001 and early fall for 2000). In each case, the correlation analysis is for the entire image subset, which includes data collected over a mixture of forest-dominated cover types. The analysis did not address correlation on an individual cover type or specific forest condition basis because of time and data constraints.

Another shortcoming in this analysis was the frequent cloud cover, even on the available Hyperion data. The July 24, 2001, scene had cloud cover in the vicinity of the heaviest defoliation areas, which was unfortunate given that most of the cloud-free defoliation areas on the image showed varying degrees of refoliation. The October Hyperion scene was not assessed for correlation because the dataset did not contain several NIR bands. Fortunately, the July 24, 2001, Hyperion data included all of the bands needed to perform simulations of both MODIS and VIIRS data.

5.2 Detecting Gypsy Moth Defoliation from MODIS-Simulated VIIRS Data

5.2.1 Visual Detection of Gypsy Moth Forest Defoliation on MODIS-simulated VIIRS Data

Based on comparison to reference data, gypsy moth defoliation patches were evident on screen displays of multitemporal color composites derived from MODIS and simulated VIIRS vegetation index data. Reference data included screen displays of Landsat and ASTER data, USFS sketch maps of gypsy moth defoliation, and publications discussing use of Landsat and/or SPOT data for mapping gypsy moth defoliation (e.g., Muchoney and Haack, 1994; Hurley et al., 2004; Townsend et al., 2004; and Hall et al., 2006).

In our study, extensive defoliation patches were visually apparent on 250-meter MODIS, 400-meter simulated VIIRS, and 500-meter MODIS NDVI products. Defoliation patches were also visible on displays of 500-meter NDMI data. The apparent defoliation patches on all of these products necessitated adoption of a specialized temporal processing method (e.g., maximum NDVI during the peak defoliation time frame). Figure 4 shows a MOD02-based RGB color composite with maximum NDVI for the peak defoliation time frame across all years in the red color gun plus the maximum NDVI peak defoliation time frame during 2001 for the blue and green guns. The deeper red tones depict defoliation. The use of this maximum NDVI enabled cloud-free imagery to be composited and compared.

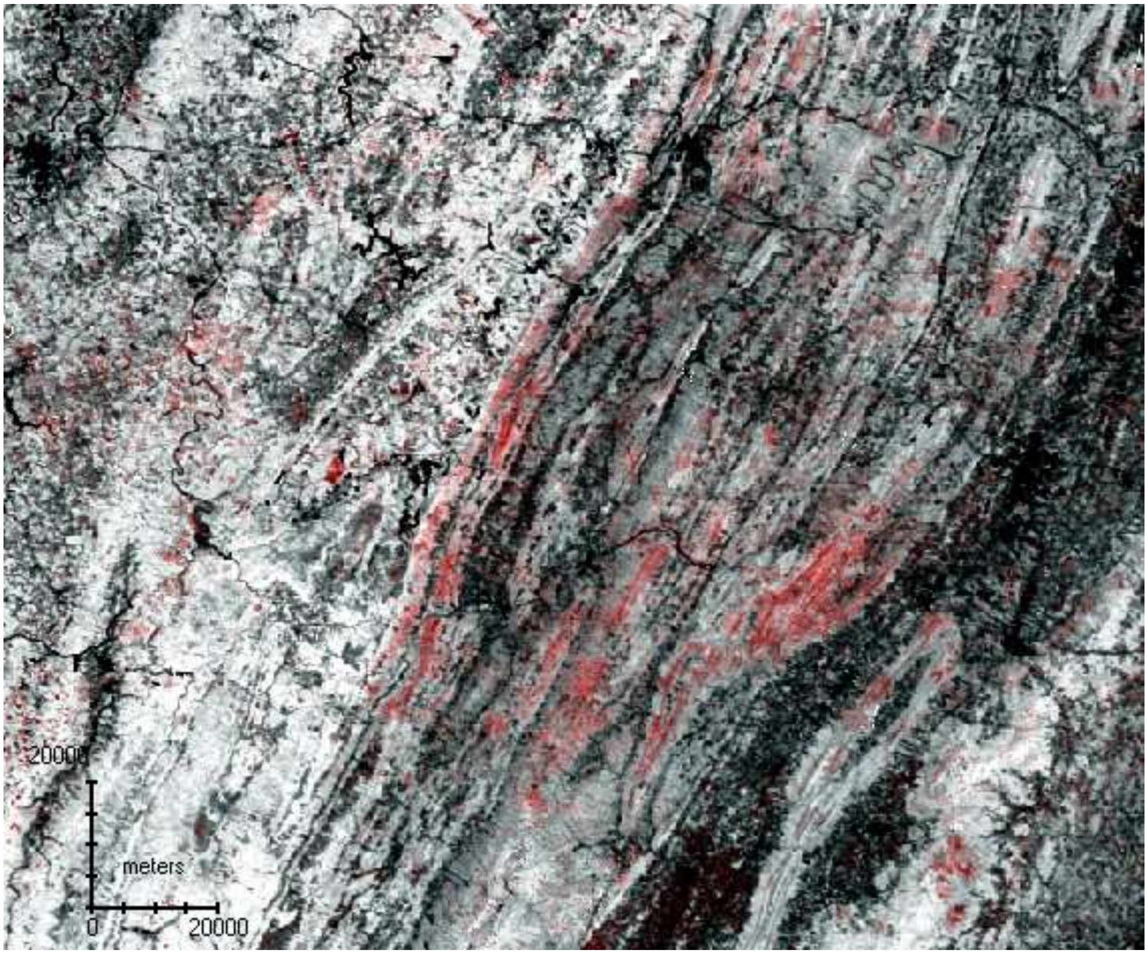

Figure 4. Synoptic visualization of 2001 gypsy moth defoliation using RGB color composite image composed of MOD02 maximum NDVI during peak defoliation across 2000–2006 in red plus maximum NDVI during peak defoliation for 2001 in blue and green. The deep red tones indicate defoliation.

RGB 2-date displays were produced with maximum NDVI for the peak defoliation time frame across all years in red gun, with maximum NDVI peak defoliation time frame during 2000 for green gun, and with maximum NDVI peak defoliation time frame during 2001 for blue gun. Doing so enable defoliation patterns of 2 consecutive years, including stands defoliated 2 years in row. The latter are at higher risk of mortality than stands with only a single year of defoliation.

5.2.2 Unsupervised Classification of Gypsy Moth Forest Defoliation from MODIS-simulated VIIRS Data

Multitemporal simulated VIIRS and MODIS Terra data both produced general land cover classifications that included non-forest, forest, and defoliated forest as categories. Table 3 show the results of unsupervised classifications of defoliated forest versus other land cover for the VIIRS 400-meter NDVI, MOD02 250-meter NDVI, MOD13 250-meter NDVI, and MOD02 500-meter NDVI, and MOD02 500-meter NDMI data, respectively. This table provides estimates of per-class producer accuracies, user accuracies, and kappa statistic values for each classification. Table 3 also provides estimates of overall accuracy and a kappa statistical value for the overall classification.

Table 3. Agreement of MODIS-simulated VIIRS and MODIS-based defoliation classifications compared to interpretation of randomly sampled locations on Landsat and ASTER RGB displays.

	Defoliated Forest			Other			Overall	
Product	**PA**	**UA**	**Kappa**	**PA**	**UA**	**Kappa**	**OA**	**OK**
VIIRS NDVI 400-m Unsupervised Classification (Simulated from MOD02)	85.96 (49/57)	77.78 (49/63)	0.67	87.93 (102/116)	92.73 (102/110)	0.78	87.28 (151/173)	0.72
MOD02 NDVI 250-m Unsupervised Classification	91.23 (52/57)	77.61 (52/67)	0.67	87.07 (101/116)	95.28 (101/106)	0.86	88.44 (153/173)	0.75
MOD13 NDVI 250-m Unsupervised Classification	43.86 (25/57)	86.21 (25/29)	0.79	96.55 (112/116)	77.78 (112/144)	0.33	79.13 (137/173)	0.46
MOD02 NDVI 500-m Unsupervised Classification	70.18 (40/57)	81.63 (40/49)	0.73	92.24 (107/116)	86.29 (107/116)	0.48	84.97 (147/173)	0.65
MOD02 NDMI 500-m Unsupervised Classification	59.65 (34/57)	79.07 (34/43)	0.69	92.24 (107/116)	82.31 (107/130)	0.46	81.50 (141/173)	0.55

Note: PA = % Producer's Agreement (# correct/total), UA = % User's Agreement (# correct/total), Kappa = Kappa Statistic, OA = % Overall Agreement (# correct/total), and OK = Overall Kappa.

The results of the 2-class classification comparisons indicate that the MOD02-simulated VIIRS 400-meter NDVI classification produced a similar yet slightly lower overall accuracy (87.28 percent with 0.72 Kappa) to the MOD02 250-meter NDVI classification (88.44 percent with 0.75 Kappa). The MOD13 250-meter NDVI classification had a lower overall accuracy (79.13 percent) and a much lower Kappa (0.46). The MOD02 500-meter NDVI classification produced a similar although slightly lower overall accuracy (84.97 percent) and Kappa (0.65) compared to the MOD02 250-meter NDVI. The MOD02 500-meter NDMI (81.5 percent overall accuracy and 0.55 Kappa) did not perform as well as the MOD02 500-meter NDVI, apparently due to residual cloud-induced noise artifacts sometimes seen in the NDMI product displays yet not evident on the NDVI products. This NDMI classification result should improve through reprocessing of the SWIR data using different settings for the TSPT software. However, time did not allow further assessment of the NDMI.

In terms of defoliation detection, the VIIRS 400-meter NDVI, MOD02 250-meter NDVI, and MOD02 500-meter NDVI showed good user and producer accuracies (≥70 percent) and acceptable Kappa values (≥0.67). The MOD13 250-meter NDVI classification yielded low producer accuracy (43.86 percent) yet a high user accuracy (86.21 percent), meaning that it usually omitted defoliation areas but did not over-classify (i.e., cause commission error) defoliation areas very much. The MOD13 result also showed the highest Kappa (0.79) in detecting defoliation. Compared to MOD02 500-meter NDVI, the MOD02

500-meter NDMI also showed lower producer accuracy (59.65 percent), similar yet slightly lower user accuracy (79.07 percent), and slightly lower Kappa (0.69) for the defoliation class.

In terms of detecting non-defoliated areas (other), all of the classifications shown in Table 3 yielded good user accuracy values (≥ ~88 percent) and producer accuracy (≥77 percent), although high Kappa values were noted only for the VIIRS 400-meter NDVI (0.78 Kappa) and MOD02 250-meter NDVI (0.86 Kappa) classifications. The MOD13 250-meter NDVI and the MOD02 500-meter NDMI showed low to mid-range Kappa values for the non-defoliated other class with ~0.33 and 0.46, respectively. The MOD02 500-meter NDVI had a midrange Kappa value of ~0.48. Kappa values can range between 0 and 1. Higher Kappa values are less likely due to random chance effects.

Temporal processing of the MODIS and VIIRS data enabled classified detection of large defoliation patches. In this case, the cloud cover was at a low enough frequency to be mitigated through temporal processing (e.g., compositing and filtering). Overall, temporal processing enabled a cloud-free, maximum-value NDVI or NDMI to be composed for each year's peak defoliation time frame, although noise from atmospheric contamination was sometimes evident. The fact that cloud-free temporal composites for the peak defoliation period could be performed with an area such as the mid-Appalachian highlands is encouraging, given that this area is frequently cloudy when gypsy moth defoliation occurs. Williams and Nelson (1986) reported that the Eastern United States is often ≥50 percent cloudy during the summer months. Even after time series data processing, residual atmospheric contamination from clouds and from cloud shadows sometimes lowered detection ability, more so in some years than others.

Producing comparable results using single-data imagery would be very difficult given the cloud statistics and the variability of average sensor zenith angle for the MODIS imagery. Many of the better MODIS scenes across the time series collected at high sensor zenith angles, which effectively increases the PSF and decreases the spatial resolution. Cloud problems were mitigated by use of temporal processing techniques on data collected when the maximum gypsy moth defoliation tends to occur (defined in this study as ~June 10–July 27 for the study area). The TSPT software identifies and removes suspected poor-quality data degraded by atmospheric contamination and poor viewing geometry. Removal of the "contaminated" data was a necessary step in producing essentially temporal, cloud-free image composites of the study area during the peak defoliation period for each year in the time series.

The results indicate that unsupervised classification of simulated VIIRS and MODIS data can identify only one intensity level of defoliation, a class that includes heavy defoliation (≥50 percent) and perhaps moderate defoliation (31–50 percent). The defoliation patches of simulated VIIRS and MODIS data do not appear to show moderate versus heavy defoliation as compared to USFS sketch maps. The sketch maps of defoliation appeared to overestimate defoliation extent compared to defoliation evident on Landsat and ASTER data screen displays. The sketch maps also omitted some defoliation. The 2003 sketch maps omitted some extensive patches of defoliated forest apparent on the MODIS and simulated VIIRS data (Figure 5). This defoliation was later confirmed qualitatively by visualization of 2003 Landsat data also acquired during the peak defoliation time frame (Figure 6).

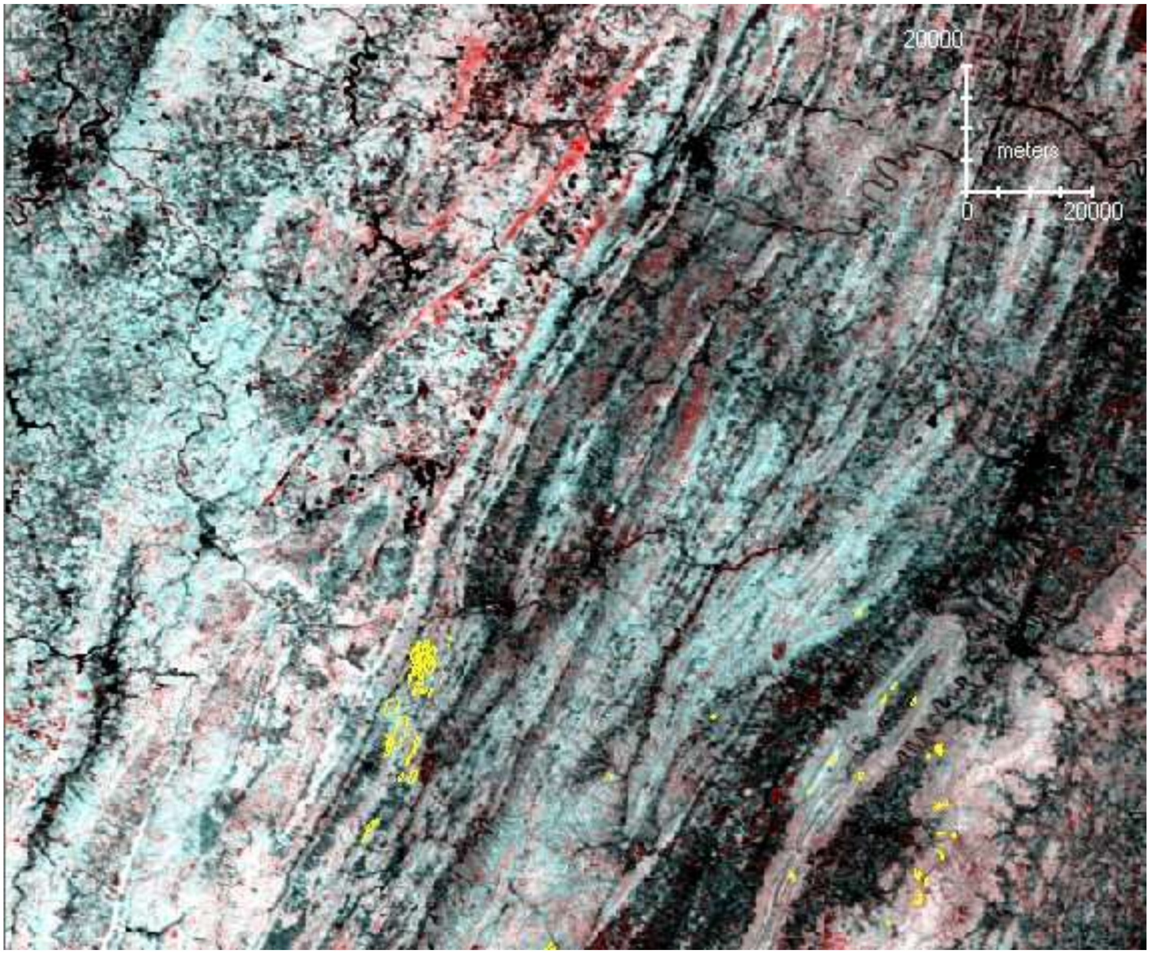

Figure 5. RGB composed of MOD02 maximum NDVI during peak defoliation across 2000–2006 loaded in red color, plus maximum NDVI during peak defoliation of 2003 assigned to the blue and green guns. The red tones of top center indicate defoliation. USFS 2003 gypsy moth defoliation sketch map areas are outlined in yellow.

Simulated VIIRS and MODIS classification products appeared to be less effective in distinguishing smaller patches of defoliation patches. In comparing results across the different years of the time series, the VIIRS and MODIS defoliation mapping products were most effective for years when defoliation was extensive, such as 2001. While results indicated that MODIS and MODIS-simulated VIIRS data produced 2001 defoliation maps in general agreement with reference data, more accuracy assessment is needed for the other years to confirm consistency of the detection techniques and suitability of the data.

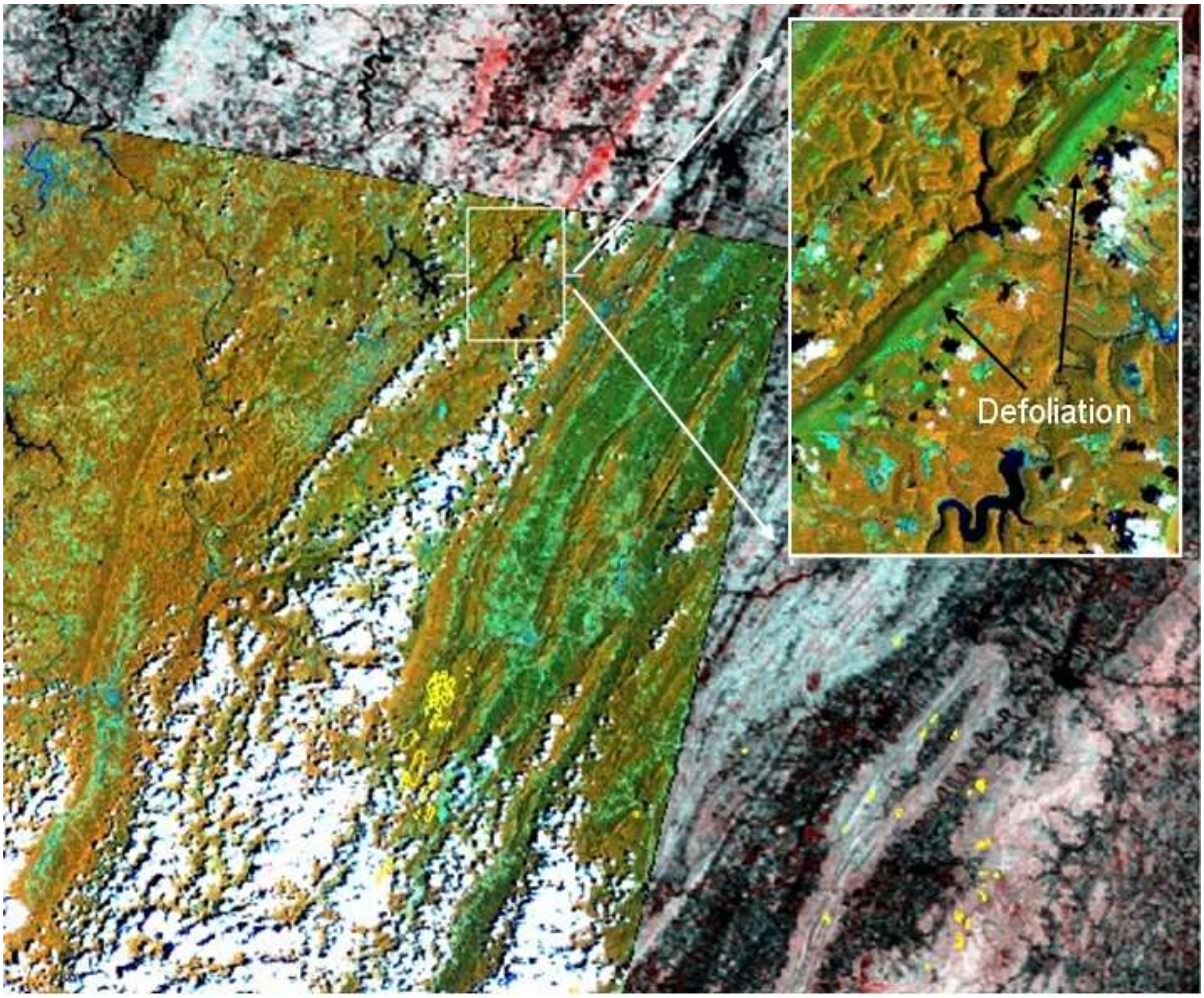

Figure 6. Landsat RGB shown in foreground is overlain onto the MODIS image shown in Figure 5. This Landsat scene was acquired on July 13, 2003, during the peak defoliation time frame. The RGB is composed of band 4 in red, band 5 in green, and band 3 in blue. The greenish tones on the Landsat RGB inset enlargement indicate defoliation.

5.2.3 Automated Defoliation Detection from MODIS-simulated VIIRS Data in Conjunction with NDVI Anomaly Detection Techniques

Automated defoliation detection from simulated VIIRS and MOD02 time series was also performed using percent change in maximum NDVI for a peak defoliation period during 2001 compared to maximum NDVI across the entire 2000–2006 time frame. Table 4 reports the map accuracy (i.e., agreement) of the 2001 simulated VIIRS and MOD02-based automated defoliation detection products and also the 2001 USFS sketch map of defoliation compared to interpretation of randomly sampled locations on Landsat and ASTER RGB screen displays.

Table 4. Agreement of MODIS-simulated VIIRS and MODIS-based automated detection defoliation maps compared to interpretation of randomly sampled locations on Landsat and ASTER RGB displays.

Product	Defoliated Forest			Other			Overall	
	PA	UA	Kappa	PA	UA	Kappa	OA	OK
VIIRS NDVI 400-m Automated Defoliation Detection: v2	73.68 (42/57)	80.77 (42/52)	0.71	91.38 (106/116)	87.60 (106/121)	0.62	85.55 (148/173)	0.67
MOD02 NDVI 250-m Automated Defoliation Detection	84.21 (48/57)	78.69 (48/61)	0.68	88.79 (103/116)	91.96 (103/112)	0.76	87.28 (151/173)	0.72
Defoliation from USFS Sketch Map	73.47 (36/49)	66.67 (36/54))	0.46	76.62 (59/77)	78.67 (59/75)	0.47	73.64 (95/129)	0.47

Note: PA = % Producer's Agreement (# correct/total), UA = % User's Agreement (# correct/total), Kappa = Kappa Statistic, OA = % Overall Agreement (# correct/total), and OK = Overall Kappa.

The automated defoliation detection products from simulated VIIRS and MOD02 data showed similar, relatively high overall classification accuracy (85.55 percent for the VIIRS 400-meter NDVI versus 87.28 percent for the MOD02 250-meter NDVI (Table 4). In contrast, the USFS aerial sketch map of gypsy moth defoliation showed a lower overall classification accuracy at 73.64 percent. The overall classification Kappa values were also similar for the VIIRS (~0.67 Kappa) versus the MOD02 (~0.72 Kappa) automated defoliation detection product, which was much higher than that exhibited by the USFS sketch map product (overall Kappa of ~0.47).

The 400-meter VIIRS and MOD02 250-meter NDVI automated detection products provided similar, good accuracy values for the defoliated forest class. In particular, the VIIRS showed a producer accuracy of 73.68 percent and a user accuracy of 80.77 percent, whereas the MOD02 product yielded producer and user accuracies of 84.21 percent and 78.69 percent, respectively. The USFS defoliation sketch map produced similar producer accuracy to the VIIRS product for the defoliated forest class with 73.47 percent but lower user accuracy for this class (66.67 percent) than the VIIRS and MOD02 automated detection products. The USFS sketch map product showed more commission error (i.e., false positives) in detecting defoliated forest than the automated detection products. The USFS sketch map showed the lowest Kappa value for the defoliated forest class with ~0.47 compared to 0.71 for simulated VIIRS and 0.68 for the MOD02 product.

The automated detection products also yielded higher accuracy values in detecting the "other" class. The VIIRS and MOD02 products showed similar producer accuracies (91.38 percent and 88.79 percent, respectively) as well as similar user accuracies (88.79 percent and 91.96 percent, respectively). However the MOD02 product's "other" class showed a higher Kappa (~0.76) compared to the VIIRS product (~0.62 for the "other" class). The USFS defoliation sketch map yielded the lowest accuracy numbers for the "other" class with 76.62 percent producer accuracy, 78.67 percent user accuracy, and a 0.47 Kappa.

Simulated VIIRS and MODIS multitemporal data also enabled an automated means to map gypsy moth defoliation via computation of percent change in maximum NDVI during the peak defoliation period for a given year compared to the maximum NDVI during peak defoliation across the entire time series of 2000–2006. Qualitative analysis of this metric for 2001 indicated that drops in forested area maximum NDVI of 4 percent or more equaled defoliation. However, this comparative analysis needs to be assessed further and then repeated for years other than 2001. The comparison technique was successful because the maximum NDVI during peak defoliation across the time series included years with and without gypsy moth defoliation. This technique holds promise for use in addressing nowcasting needs of the forest threat EWS. This approach also enabled a means to quantify and assess relative defoliation intensity.

5.2.4 Additional Discussion of Results

Good potential exists for improved exploitation of vegetation index time series data, especially in eliminating cloud contamination to compute vegetation indices via temporal noise filtering and gap interpolation. Atmospheric correction of reflectance is highly desirable for detection and depiction of vegetation anomalies from NDVI time series, although the products need to be as near real time as possible for fullest use in the EWS. Improvements in atmospheric correction of specific MODIS and VIIRS data products may improve detection capabilities if it doesn't add noise, especially in areas such as the mid-Appalachian highlands where cloud cover is frequent during the relatively narrow time frame of peak gypsy moth defoliation. Cloud cover was frequent enough to negate the full potential use of single-day composites for characterizing the defoliation process on a daily basis. However, useful products were obtained by extracting the maximum NDVI across the peak defoliation time frame for each year and for the same time frame across the entire time series. While atmospherically corrected products may be desirable, the most useful products for this RPC experiment were from MOD02 products that were not atmospherically corrected.

Improved processing (e.g., noise reduction) may enable improved development of defoliation detection maps using other NDVI derivative products in addition to maximum NDVI. For example, improvements in defoliation detection could occur through combined use of minimum NDVI over the peak defoliation time frame for a given year in conjunction with the maximum NDVI during peak defoliation across the entire time series. This technique was tried but was not effective because of the noisiness of the minimum-value NDVI imagery within the peak defoliation time frame. However, better noise reduction could make this technique more useful. A more effective computation of minimum NDVI values during the peak defoliation time frame would also be helpful for improving computation of average NDVI across the same time frame.

Use of vegetation index alternatives to NDVI may also improve detectability of gypsy moth defoliation. Multitemporal NDVI and NDMI both showed defoliation areas in the study area during 2001, although the NDVI appeared to be less noisy and showed defoliation slightly better. The NDMI product showed noise not evident in the NDVI products yet appeared to show defoliation quite well (maybe better than NDVI) for the non-noise influenced areas. The NDMI product could well be improved by reprocessing to reduce noise in the SWIR band imagery used as an input to NDMI. The MODIS NDVI product at 250-meter resolution was twice as spatially resolute as the NDMI product at 500-meter pixels. However, MOD02 250-meter and 500-meter NDVI data products enabled comparable displays and classifications of gypsy moth-induced forest defoliation. Other factors, such as forest disturbance type, defoliation intensity, forest ground cover, and weather conditions, may also affect detectability of defoliation from either NDVI or NDMI. VIIRS will have an SWIR band at 400-meter resolution, which made it impractical to use of MODIS for VIIRS NDMI computation although MODIS NDMI at 500 meters is at least a spatially similar proxy.

The project focused on use of data from MODIS Terra as opposed to MODIS Aqua mainly because only MODIS Terra data was collected during 2000 and 2001: years with comparatively high amounts of gypsy moth defoliation within the study area. In addition, sufficient Landsat and ASTER data was collected during the 2001 peak defoliation time frame to enable quantitative accuracy assessment of MODIS and simulated VIIRS products. MODIS Aqua data became available in 2002, which precluded its use during the year with the best reference data. Time and budget constraints prohibited the evaluation of MODIS Aqua or fused Aqua/Terra products.

Use of Aqua products may be more realistic for VIIRS simulation than use of Terra products because Aqua acquires data at the same time of day as is projected for NPP (NPOESS Preparatory Project) VIIRS (Privette et al., 2007). Use of fused MODIS Terra and Aqua products may improve the results by mitigating cloud cover contamination frequency and by improving defoliation detection accuracy. During part of the VIIRS era, multiple VIIRS systems should be in operation so that each ground area would be imaged at least twice during daylight hours as with the MODIS Aqua and Terra.

5.3 Gaps in Meeting Needs of Forest Threat EWS

5.3.1 Gaps Regarding Data Simulation Validation

A concerted effort was made to assess the potential of VIIRS NDVI products for meeting needs of the forest threat EWS, although information gaps remained upon completion of the experiment. In particular, efforts were made to provide the most realistic simulated VIIRS data possible given time, resource, and knowledge constraints. The simulation of VIIRS data required multiple software modifications to produce refined, realistic vegetation index products. Comparisons of VIIRS simulations from MODIS and Hyperion data revealed high correlations, although comparison of additional datasets would have been helpful, especially during the peak defoliation period. Uncertainty still remains as to the simulation's realism, especially given that VIIRS specifications may be modified before launch.

5.3.2 Gaps Regarding Use of Atmospheric Correction Reflectance Products

Daily satellite-based reflectance and/or vegetation index products will be needed as an input into the USFS Forest Threat EWS. It remains unclear whether such data products must be atmospherically corrected to ground reflectance or whether planetary reflectance imagery would suffice. Attempts to use MOD09 data during this study yielded mixed results. Atmospheric correction of MOD09 products appeared to contain more visible noise that essentially muted the defoliation pattern both on RGB displays and on detection products. The noise was reduced but not eliminated though more rigorous processing of the MOD09 products (Figure 7). The noise evident in the MOD09 raw data caused significant omission for classification of defoliation areas. Because of these problems, further evaluation (e.g., accuracy assessment) of MOD09 products for this application was not pursued until a better determination could be made of the nature of the MOD09 noise artifacts. Views of non-temporally filtered MOD09 data products indicate that the noise problem is evident prior to TSPT processing. A modification of the atmospheric correction procedure may be needed to make MOD09 products more useful for this forest threat EWS application.

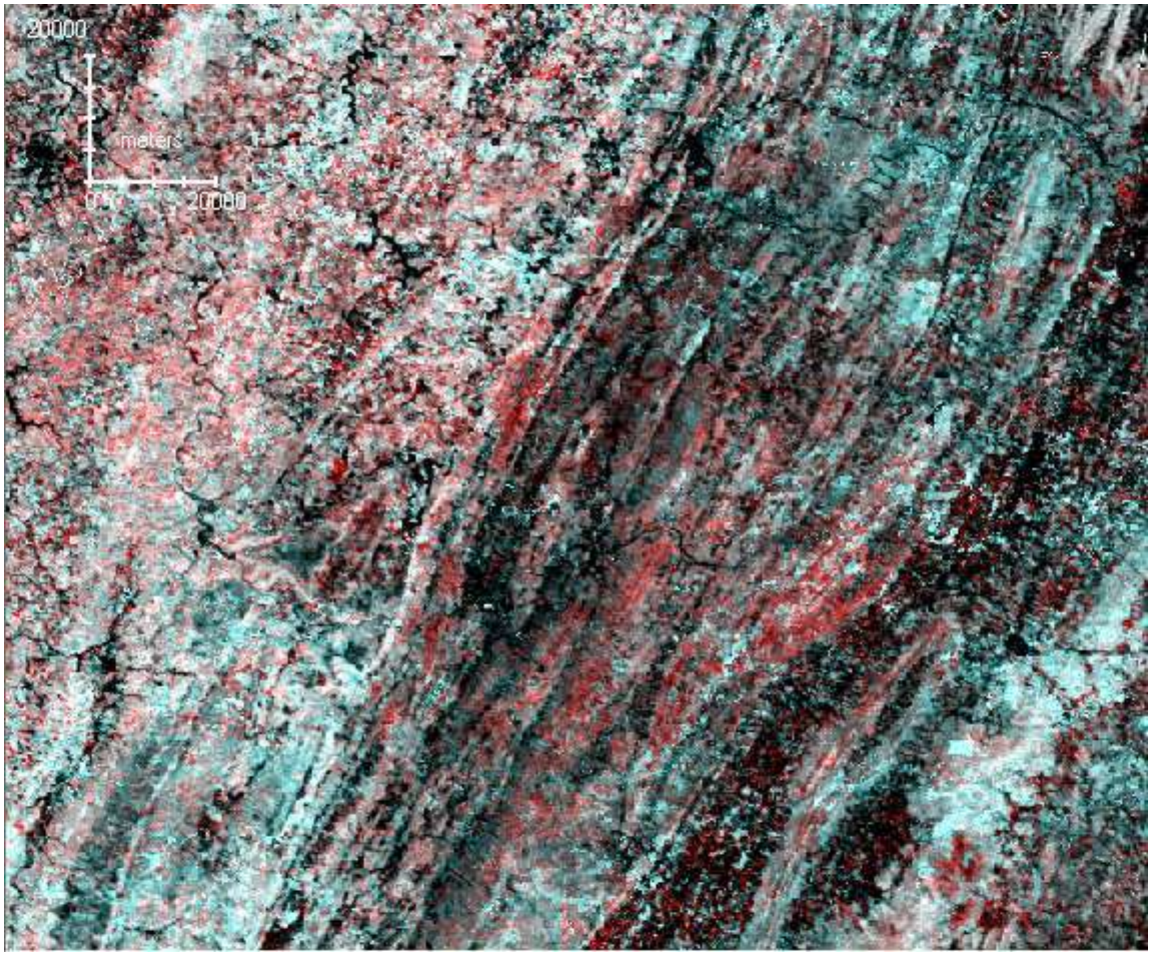

Figure 7. RGB color composite of study area computed from 250-meter MOD09 data. The image is composed of maximum NDVI over the peak defoliation time frame for 2000–2006 in the red gun, plus peak defoliation maximum NDVI for 2001 loaded into the blue and green color guns. The deep red tones indicate defoliation. Compare this image to the MOD02 RGB shown in Figure 4.

For areas prone to clouds during peak defoliation, atmospheric correction may increase noisiness of vegetation index products compared to results from MOD02 planetary reflectance. Collection 5 MOD09 atmospheric correction should enable an improved application product and may therefore help improve defoliation detection results for cloud-prone areas, such as the Mid-Appalachian Highlands. In the meantime, alternative processing strategies need to be attempted to increase the utility of the MOD09 data in mapping forest defoliation.

5.3.3 Gaps in Use of Fused MODIS Aqua/Terra Products for VIIRS Simulation

Fusion products derived from both MODIS Aqua and Terra data were tried on a limited extent; time constraints prohibited a more comprehensive study. Such products need to be explored further for gypsy moth defoliation mapping as well as suitability for VIIRS simulations. Additional VIIRS simulation work should compare MODIS Aqua data results to those from MODIS Terra. MODIS Aqua collects data during the same time of day as the NPP VIIRS, which may or may not pose an increased amount of cloud-cover problems affecting data quality.

5.3.4 Gaps in Defoliation Detection Product Validation

A more comprehensive accuracy assessment of forest defoliation detection products obtainable from MODIS and VIIRS data is needed, especially for validation of products for years other than 2001. In addition, more validation is needed for assessing the near real time potential of automated detection products via the percent maximum NDVI approach. Further analysis of the accuracy of defoliation detection products as a function of patch size would also be helpful.

6.0 Conclusions, Recommendations, and Next Steps

The results of the RPC experiment indicate that VIIRS and MODIS data products have good potential for integration into the forest threat EWS. In particular, both simulated VIIRS and MODIS data were processed into gypsy moth forest defoliation products that compared well to Landsat and ASTER imagery collected during the peak defoliation time frame. These results were demonstrated and validated for the 2001 gypsy moth defoliation season, but doing so required that multitemporal data be processed over the entire MODIS time series from 2000–2006. This processing was needed to construct a basis for comparing maximum NDVI conditions from a given gypsy moth defoliation season to the maximum NDVI for the same season across the whole time series.

Additional work (e.g., quantitative accuracy assessment) should be performed to further assess gypsy moth defoliation detection products derived from both MODIS and simulated VIIRS data processing. In particular, additional years of apparent defoliation detections need to be assessed quantitatively for years other than 2001. Further validation work is needed to assess accuracy of other years (e.g., 2000 and 2003) in which apparent defoliation is most prevalent on the VIIRS and MODIS products.

The RPC project focused on the ability of VIIRS data to monitor only one example of a major invasive forest damaging insect. In addition, other forest threats of similar magnitude may be detected and tracked at MODIS and VIIRS scales. Gypsy moth is one of eight major biotic forest threats identified in the HFRA legislation. Abiotic events, such as severe storm damage and anthropogenic activities (e.g., urbanization), also can negatively impact and threaten forest ecosystems. Many forest threats are ecosystem and/or regionally specific. Ideally, threat detection strategies, like forest threat risk maps, need to be tailored for specific threats, ecosystems, and regions. The more episodic disturbances, such as incidental forest defoliation from insect attack, would especially benefit from such tailoring.

Other detection techniques should also be evaluated to assess the applicability of VIIRS products for forest threat detection. In addition to NDVI- and NDMI-based techniques, other band ratio, data transformation, or statistical approaches may also need to be evaluated before adoption, depending on the forest threat, landscape characteristics, and cloud cover frequency of the study area. Future work should also consider use of multitemporal, satellite-based temperature data as an input to the forest threat EWS because temperature can play an important role in insect-induced forest damage. For example, mountain pine beetle forest damage risk is in part related to seasonal temperature patterns (Logan and Powell, 2005).

While MODIS and VIIRS data products were useful for computing gypsy moth defoliation maps, they were deployed in hindcast mode. The use of such products needs to be tried for nowcasts of gypsy moth defoliation. Doing so will require use of historic time series data of previous years and also of a contiguous sequence of days before a given current date. In essence, a latest pixel composite of maximum NDVI going back 1 week from the present would need to be constructed in near real time and then compared to the maximum NDVI for the same time frame. Additional work needs to be done to explore the use of near real time NDVI anomaly detection concerning gypsy moth defoliation.

The RPC project considers one extensive study area (mid-Appalachian Highlands) that is not completely representative of all forest landscapes and U.S. regions with extensive forest. Other forest types and landscape conditions should also be analyzed for vulnerability to major insect threats, including those in coastal and inland areas.

The project demonstrated and validated a means to monitor forest defoliation with simulated VIIRS and MODIS time series data. Such ability to track forest disturbances from insect outbreaks is important to those studying forest pest dynamics, especially in regard to climate change (Logan et al., 2003; Breshears et al., 2005; Logan and Powell, 2005). Forest pest dynamics can be related to other kinds of disturbance, such as fire (Logan et al., 2003) and also hurricane damage (Hunter, 2002). The technological gains made in this experiment should be applied to other forest sustainability concerns, such as the relationship of climate change to forest disturbance and sustainability. Publication of results from this experiment will inform the USFS and the related forest health assessment community about this study. Future work in the near term will include presenting results from the experiment at conferences and developing a manuscript for journal publication.

7.0 References

Blonski, S., G. Gasser, J. Russell, R. Ryan, G. Terrie, and V. Zanoni, 2002. Synthesis of multispectral bands from hyperspectral data: Validation based on images acquired by AVIRIS, Hyperion, ALI, and ETM+. In *Proceedings of 11th JPL AVIRIS Geoscience Workshop*, March 4–8, 2002.

Bosworth, D., 2006. Statement of Dale Bosworth, Chief, U.S. Forest Service, United States Department of Agriculture Before the United States Senate, Committee on Energy and Natural Resources, Subcommittee on Public Lands and Forests Concerning Healthy Forests Restoration Act Implementation, July 19, 2006, online at: http://energy.senate.gov/public/index.cfm?FuseAction=Hearings.Testimony&Hearing_ID=1574&Witness_ID=1426 (last accessed August 16, 2006).

Brewer, K., B. Ruefenacht, and M. Finco, 2005. Development and production of a moderate resolution forest type map of the United States. Presentation, Forest Health Risk Mapping Workshop: Quantitative Techniques for Deriving National-Scale Data, USDA Forest Service, Forest Health Technology Enterprise Team, Publication FHTET-05-12, online at: http://www.fs.fed.us/foresthealth/technology/pdfs/Brewer.pdf, accessed July 22, 2007.

Breshears, D.D., N.S. Cobb, P.M. Rich, K.P. Pricee, C.D. Allen, R.G. Balice, W.H. Romme, J.H. Kastens, M.L. Floyd, J. Belnap, J.J. Anderson, O.B. Myers, and C.W. Meyer, 2005. Regional vegetation die-off in response to global-change-type drought. *Proceedings of the National Academy of Sciences U.S.A.* 102(42):15144–15148; online at http://www.pnas.org/cgi/reprint/102/42/15144, accessed August 15, 2007.

Chornesky, E.A., A.M Bartuska, G.H. Aplet, K.O. Britton, J. Cummings-Carlson, F.W. Davis, J. Eskow, D.R. Gordon, K.W. Gottschalk, R.A. Haack, A.J. Hansen, R.N. Mack, F.J. Rahel, M.A. Shannon, L.A. Wainger, and T.B. Wigley, 2005. Science priorities for reducing the threat of invasive species to sustainable forestry. *BioScience* 55(4):335–348.

Ciesla, W.M., 2000. *Remote Sensing in Forest Health Protection*. FHTET Report No. 00-03, U.S. Department of Agriculture, Forest Service, Forest Health Technology Enterprise Team, Remote Sensing Applications Center, 266 p., online at: http://www.fs.fed.us/foresthealth/technology/pdfs/RemoteSensingForestHealth00_03.pdf.

Dale, V.H., L.A. Joyce, S. McNulty, R.P. Neilson, M.P. Ayres, M.D. Flannigan, P.J. Hanson, L.C. Irland, A.E. Lugo, C.J. Peterson, D. Simberloff, F.J. Swanson, B.J. Stocks, and W.B. Wotton, 2001. Climate change and forest disturbance. *BioScience* 51(9):723–734.

Committee on Ocean Policy, 2007. *U.S. Ocean Action Plan Implementation Update.* Council on Environmental Quality, January 26, 57 pp., online at: http://ocean.ceq.gov/oap_update012207.pdf, accessed August 14, 2007.

Ellenwood, J., 2006. *Forest Health Monitoring – Enhancing Detection Monitoring*. Presentation, US Forest Service Forest Disturbance Mapping Workshop, Salt Lake City, Utah, November 29, 2006.

FICMNEW [Federal Interagency Committee for Management of Noxious and Exotic Weeds], 2003. *A National Early Detection and Rapid Response System for Invasive Plants in the United States: Conceptual Design*, 24 p., online at: http://www.fws.gov/ficmnew/FICMNEW_EDRR_FINAL.pdf, accessed July 13, 2007.

Hall, R.J., R.S. Skakun, and E.J. Arsenault, 2006. Remotely sensed data in the mapping of insect defoliation. Chapter 4 in *Understanding Forest Disturbance and Spatial Pattern: Remote Sensing and GIS Approaches* (M.A. Wulder and S.E. Franklin, eds.), Taylor and Francis, CRC Press, Boca Raton, Florida, USA, pp. 85–111.

Hargrove, W.W., and F.M. Hoffman, 2006. *The Forest Incidence Recognition and State Tracking (FIRST) System: A Prototype Forest Threat Detection System*. Internal Proposal from the Department of Energy Oak Ridge National Laboratory to the USDA Forest Service, 6 p.

Hayes, D.J., W. Cohen, S.A. Sader, and D.E. Irwin, in press. Estimating proportional change in forest cover as a continuous variable from multi-year MODIS data. *Remote Sensing of Environment* (in press).

Hayes, D.J., and W.B. Cohen, 2007. Spatial, spectral and temporal patterns of tropical forest cover change as observed with multiple scales of optical satellite data. *Remote Sensing of Environment* 106(1):1–17.

Hunter, M.D., 2002. Ecological causes of pest outbreaks. In *Encyclopedia of Pest Management* (D. Pimentel, ed.), Marcel Dekker, Inc., pp. 214–217, online at: http://www.arches.uga.edu/~mdhunter/publications/encyclopedia.pdf, accessed July 28, 2007.

Hurley, A., D. Watts, B. Burke, and C. Richards, 2004. Identifying gypsy moth defoliation in Ohio using Landsat data. *Environmental and Engineering Geoscience* 10: 321–328.

Jin, S., and S.A. Sader, 2005a. MODIS time-series imagery for forest disturbance detection and quantification of patch size effects. *Remote Sensing of Environment* 99: 462–470.

Jin, S., and S.A. Sader, 2005b. Comparison of time-series tasseled cap wetness and the normalized difference moisture index in detecting forest disturbances. *Remote Sensing of Environment* 94(3):364–372.

Kharuk, V.I., K.J. Ranson, A.G. Kozuhovskaya, Y.P. Kondakov, and I.A. Pestunov, 2004. NOAA/AVHRR satellite detection of Siberian silkmoth outbreaks in eastern Siberia. *International Journal of Remote Sensing* 25: 5543–5555.

Krist, F., 2007. Mapping risk from forest insects and diseases. Presentation, 2007 Forest Stewardship Program Spatial Analysis Summit, online at: http://www.fs.fed.us/na/sap/downloads/summit/05%20Krist_RiskMap_041907.pdf, accessed July 22, 2007.

Lewis, J.W., 2002. Mapping Risk from Forest Insects and Diseases. Report FS-754, Washington DC: U.S. Department of Agriculture, Forest Service, 60 p., online at: http://www.fs.fed.us/foresthealth/publications/Mapping%20Risk.pdf.

Lin, H., J. Brown, and J. Verdin, 2006. USGS drought activities. Presentation, NIDIS Draft Implementation Plan Workshop, Longmont, CO, September, 21-22, 2006, online at: http://www.joss.ucar.edu/joss_psg/meetings/Meetings_2006/nidis/presentations/Verdin.pdf, accessed July 13, 2007.

Logan, J.A., and J.A. Powell, 2005. Ecological consequences of climate change altered forest insect disturbance regimes. In *Climate Change in Western North America: Evidence and Environmental Effects* (F.H. Wagner, ed.), Allen Press (in review), online at: http://www.usu.edu/beetle/documents/Logan-Powell2005.pdf, accessed July 22, 2007.

Logan, J.A., J. Régnière, D.R. Gray, and A.S. Munson, 2007. Risk assessment in the face of a changing environment: Gypsy moth and climate change in Utah. *Ecological Applications* 17(1):101–117.

Logan, J.A., J. Régnière, and J.A. Powell, 2003. Assessing the impacts of global climate change on forest pests. *Frontiers in Ecology and the Environment* 1: 130–137.

McKellip, R., R.E. Ryan, D. Prados, and S. Blonski, 2005. Crop surveillance demonstration using a near-daily MODIS vegetation index time series. In 2005 International Workshop on the Analysis of Multi-Temporal Remote Sensing Images, New York City: IEEE.

Muchoney, D.M., and B.N. Haack, 1994. Change detection for monitoring forest defoliation. *Photogrammetric Engineering & Remote Sensing* 60(10):1243–1251.

Morin, R.S., A.M. Liebhold, E.R. Lister, K.W. Gottschalk, and D.B. Twardus, 2004. *Mapping Host-Species Abundance of Three Major Exotic Forest Pests*. Research Paper NE-726, Newtown Square, PA: U.S. Department of Agriculture, Forest Service, Northeastern Research Station, 11 p., online at: http://www.fs.fed.us/ne/newtown_square/publications/research_papers/pdfs/2005/ne_rp726.pdf.

Morrissey, W.A., 2006. *Tsunamis: Monitoring, Detection, and Early Warning Systems*. Congressional Research Service, The Library of Congress, 24 p., online at: http://www.italy.usembassy.gov/pdf/other/RL32739.pdf, accessed July 13, 2007.

Nielson, E., B. Quayle, and J. Johnson, 2006. USFS RSAC work in broad-scale forest change detection. 2006 USDA Forest Service Workshop on Forest Disturbance Mapping.

Nielson, E., and M. Finco, 2006. First pass flowchart of disturbance monitoring process. Presentation, 2006 USDA Forest Service Workshop on Forest Disturbance Mapping.

Pimentel, D., L. Lach, R. Zuniga, and D. Morrison, 2000. Environmental and economic costs associated with non-indigenous species in the United States. *BioScience* 50(1):53–65.

Potter, C., T. Pang-Ning, V. Kumar, C. Kucharik, S. Klooster, V. Genovese, W. Cohen, and S. Healey, 2005. Recent history of large-scale ecosystem disturbances in North America derived from the AVHRR satellite record. *Ecosystems* 8(7):808–824.

Prados, D., R.E. Ryan, and Ross, K.W., 2006. Remote Sensing Time Series Product Tool. Poster, 2006 AGU Fall Meeting, abstract online at: http://start.org/meetings/fm06/fm06-sessions/fm06_IN33B.html (accessed June 29, 2007).

Privette, J.L., A.C. Pinheiro, and Y. Yu, 2007. Developing a long term data record of land surface temperature. Presentation, MODIS Land Collection 5/LTDR Workshop, online at: http://modis.gsfc.nasa.gov/sci_team/meetings/c5meeting/pres/ltdr/yu.pdf, accessed July 29, 2007.

Quayle, B., K. Lannom, M. Finco, J. Norton, and R. Warnick, 2003. Monitoring wildland fire activity on a national-scale with MODIS imagery. 2nd International Wildland Fire Ecology and Fire Management Congress, 5th Symposium on Fire and Forest Meteorology, 4 p., online at: http://ams.confex.com/ams/FIRE2003/techprogram/paper_66050.htm, accessed July 13, 2007.

Ramsey, E.W., III, M.E. Hodgson, S.K. Sapkota, and G.A. Nelson, 2001.Forest impact estimated with NOAA AVHRR and Landsat TM data related to an empirical hurricane wind-field distribution. *Remote Sensing of Environment* 77(3):279–292.

Ranson, K.J., V. Kharuk, and S. Im, 2006. Terra/MODIS AND SPOT VEGETATION data in monitoring Siberian silkmoth outbreaks in the mountain taiga zone. Presentation, 13th Conference of the International Boreal Forest Research Association (IBFRA), 28–30 August 2006, Umeå, Sweden.

Rojas, F., R.A. Schowengerdt, and S.F. Biggar, 2002. Early results on the characterization of the Terra MODIS spatial response. *Remote Sensing of Environment* 83: 50–61.

Ross, K., J. Russell, and R.E. Ryan, 2006. Simulating Visible/Infrared Imager/Radiometer Suite Normalized Difference Vegetation Index data using Hyperion and MODIS. Poster, 2006 AGU Fall Meeting, abstract online at: http://start.org/meetings/fm06/fm06-sessions/fm06_IN33B.html (accessed June 29, 2007).

Ryan, R., 2006. Alternative remote sensing data sources for disturbance mapping. Presentation, 2006 USDA Forest Service Workshop on Forest Disturbance Mapping.

Sader, S.A. and J.C. Winne, 1992. RGB-NDVI color composites for visualizing forest change dynamics. *International Journal of Remote Sensing* 13(16):3055–3067.

Schrader-Patton, C., 2003. *Digital Aerial Sketchmapping*. USDA Forest Service – Engineering, Forest Health Technology Enterprise Team – Fort Collins, Remote Sensing Applications Center, Report No. RSAC-1202-RPT2, 17 p.

Schueler, C., J.E. Clement, L. Darnton, F. DeLuccia, T. Scalione, and H. Swenson, 2003. VIIRS sensor performance. In *Proceedings: 2003 IEEE International Geoscience and Remote Sensing Symposium*, 21–25 July, 1: 369– 372.

Townsend, P.A., K.N. Eshleman, and C. Welcker, 2004. Remote sensing of gypsy moth defoliation to assess variations in stream nitrogen concentrations. *Ecological Applications* 14: 504–516.

United Nations, 2006. Global Survey of Early Warning Systems – An assessment of capacities, gaps and opportunities towards building a comprehensive global early warning system for all natural hazards. http://www.unisdr.org/ppew/info-resources/ewc3/Global-Survey-of-Early-Warning-Systems.pdf, United Nations, accessed June 24, 2007.

U.S. House, 2003. 108th Congress, 1st Session. *H.R. 1904, Healthy Forest Restoration Act of 2003*. 29 p., online at: http://www.fs.fed.us/biology/wildecology/HFRA.pdf, accessed July 13, 2007.

USFS [USDA Forest Service], 2004a. Western Wildland Environmental Threat Assessment Center – Center Charter, 9 p.

USFS, 2004b. *The Early Warning System for Forest Health Threats in the United States*. Final Draft, 37 p., online at: http://www.fs.fed.us/foresthealth/publications/EWS_final_draft.pdf, accessed June 29, 2007.

USFS, 2005. Eastern Forest Environmental Threat Assessment Center – Center Charter, 8 p.

USFS and Bureau of Land Management, 2004. *The Healthy Forest Initiative and Healthy Forest Restoration Act: Interim Field Guide*. Report FS-799, February 2004, 58 p., online at: http://www.fs.fed.us/projects/hfi/field-guide/documents/interim-field-guide.pdf, accessed July 13, 2007.

USFS, 2007. *Annual Gypsy Moth Defoliation*. Metadata on geospatial datasets available online at: http://www.fs.fed.us/ne/morgantown/4557/AFPE/metadata/gm_annual_defoliation.htm, accessed July 13, 2007.

USGS [U.S. Geological Survey], 2005. *An Assessment of Volcanic Threat and Monitoring Capabilities in the United States: Framework for a National Volcano Early Warning System*. USGS OPEN-FILE REPORT 2005-1164, 62 p., online at: http://pubs.usgs.gov/of/2005/1164/, accessed July 13, 2007.

USGS and NPS [National Park Service], 2007. *USGS - NPS Vegetation Mapping Program*. Online at: http://biology.usgs.gov/npsveg/aa/toc.html, accessed July 25, 2007.

Vogelmann, J.E., 1990. Comparison between two vegetation indices for measuring different types of forest damage in the Northeastern United States. *International Journal of Remote Sensing* 11: 2281–2297.

Williams, D.L., and R.F. Nelson, 1986. Use of remotely sensed data for assessing forest stand conditions in the Eastern United States. *IEEE Transactions on Geoscience and Remote Sensing* GE-24: 130–138.

Zanoni, V., B. Davis, R. Ryan, G. Gasser, and S. Blonski, 2002. Remote sensing requirements development: A simulation-based approach. *Proceedings of the ISPRS Commission I Mid-Term Symposium 2002: Integrated Remote Sensing at the Global, Regional and Local Scale*, November 10–15, 2002, Denver, CO, IAPRS Vol. XXXIV, Part 1.

This page intentionally blank

Appendix A. Acronyms

ALI	Advanced Land Imager
ART	Application Research Toolbox
ASTER	Advanced Spaceborne Thermal Emission and Reflection Radiometer
AVHRR	Advanced Very High Resolution Radiometer
EWS	Early Warning System
FIA	Forest Inventory Assessment
FIRST	Forest Incidence Recognition and State Tracking System
GIS	Geographic Information System
GPS	Global Positioning System
GSD	Ground Sampling Distance
HFRA	Healthy Forest Restoration Act
MODIS	Moderate Resolution Imaging Spectroradiometer
MRT Swath	MODIS Swath Reprojection Tool
NDMI	Normalized Difference Moisture Index
NDVI	Normalized Difference Vegetation Index
NIR	near infrared
NPOESS	National Polar-orbiting Operational Environmental Satellite System
NPP	NPOESS Preparatory Project
PSF	point spread function
RPC	Rapid Prototyping Capability
SPOT	Système Probatoire d'Observation de la Terre
SWIR	short-wave infrared
TCW	Tasseled Cap Wetness
TSPT	Time Series Product Tool
USFS	USDA Forest Service

VIIRS	Visible/Infrared Imager/Radiometer Suite

Appendix B. MODIS Products Used in RPC Experiment

Source for descriptions below (unless otherwise noted):

NASA, n.d. *MODIS Data Products*. Online at: http://modis.gsfc.nasa.gov/data/dataprod/index.php (accessed July 30, 2007).

B.1. MOD02: Level-1B Calibrated Geolocation Dataset

The Level 1B dataset contains calibrated and geolocated at-aperture radiances for 36 bands generated from MODIS Level 1A sensor counts (MOD 01). The radiances are in W/(m2-µm-sr). In addition, reflectance may be determined for the solar reflective bands (bands 1–19, 26) through knowledge of the solar irradiance (e.g., determined from MODIS solar-diffuser data and from the target-illumination geometry). Additional data are provided, including quality flags, error estimates, and calibration data.

B.2. MOD02HKM: Level-1B 500-m Calibrated Radiances

The 500-meter MODIS Level 1B dataset contains calibrated and geolocated at-aperture radiances for 7 discrete bands located in the 0.45 to 2.20 micron region of the electromagnetic spectrum. These data are generated from the MODIS Level 1A scans of raw radiance and in the process converted to geophysical units of W/(m^2 um sr). In addition, the Earth Bidirectional Reflectance Distribution Function (BRDF) may be determined for these solar reflective bands through knowledge of the solar irradiance (e.g., determined from MODIS solar diffuser data, and from the target illumination geometry). Additional data are provided including quality flags, error estimates, and calibration data. (Source: http://gcmd.gsfc.nasa.gov/records/GCMD_MOD02HKM.html)

B.3. MOD02QKM: Level-1B 250-m Calibrated Radiances

The 250-meter MODIS Level 1B dataset contains calibrated and geolocated at-aperture radiances for 2 discrete bands located in the 0.62 to 0.88 micron region of the electromagnetic spectrum. These data are generated from the MODIS Level 1A scans of raw radiance and in the process converted to geophysical units of W / (m^2 um sr). In addition, the Earth Bi-directional Reflectance Distribution Function (BRDF) may be determined for these solar reflective bands through knowledge of the solar irradiance (e.g., determined from MODIS solar diffuser data, and from the target illumination geometry). Additional data are provided including quality flags, error estimates, and calibration data. (Source: http://gcmd.gsfc.nasa.gov/records/GCMD_MOD02QKM.html)

B.4. MOD03: Geolocation Dataset

The MODIS Geolocation product contains geodetic coordinates, ground elevation, and solar and satellite zenith, and azimuth angle for each MODIS 1-km sample. These data are provided as a companion dataset to the Level 1B calibrated radiances and the Level 2 datasets to enable further processing. These geolocation fields are determined using the spacecraft attitude and orbit, instrument telemetry, and a digital elevation model.

B.5. MOD09: Surface Reflectance; Atmospheric Correction Algorithm Products

The MODIS Surface-Reflectance Product (MOD 09) is computed from the MODIS Level 1B land bands 1, 2, 3, 4, 5, 6, and 7 (centered at 648 nm, 858 nm, 470 nm, 555 nm, 1240 nm, 1640 nm, and 2130 nm, respectively). The product is an estimate of the surface spectral reflectance for each band as it would have been measured at ground level if there were no atmospheric scattering or absorption.

B.6. MOD12: Land Cover/Land Cover Change

The MODIS global land cover product (MOD12) consists of two suites of scientific datasets (SDS): MOD12Q1 (global land cover) and MOD12Q2 (global land cover dynamics). The MOD12Q1 SDS suite includes five layers depicting different global land cover classifications. The MOD12Q2 SDS suite provides seven layers that characterize seasonal time scale dynamics in ecosystems at global scale. In collection 5, both are being produced at a spatial resolution of 500-m at annual and bi-annual time-steps for MOD12Q1 and MOD12Q2, respectively.

B.7. MOD13: Gridded Vegetation Indices (NDVI & EVI)

MODIS core mission, standard VI products include the normalize difference vegetation index (NDVI) and the enhanced vegetation index (EVI) to effectively characterize biophysical/biochemical states and processes from vegetated surfaces. There exists a complete, global time series record of 6 VI products from each of the Terra and Aqua MODIS sensors, at varying spatial (250 m, 1 km, 0.05 degree) and temporal (16-day, monthly) resolutions to meet the needs of the research and application communities. The VI products are validated with accuracies depicted by a pixel reliability flag and with globally averaged uncertainties of 0.015 units.

B.8. MOD35: Cloud Mask

The MODIS cloud mask product indicates whether a pixel is unobstructed between the surface and satellite. The product provides 48 bits of output per 1-km pixel that includes information on sets of multispectral test results (from 19 MODIS spectral bands), the decision tree used to arrive at the product, and limited ancillary information such as a land/ocean and snow/no snow flags. The first eight bits provide a summary sufficient for most applications. Additionally, the first two bits simply offer information in four categories: confident clear, probably clear, uncertain/probably cloudy, and cloudy.

B.9. MOD43: Surface Reflectance BRDF/Albedo Parameter

Surface albedo is one of the key radiation parameters required for modeling of the Earth\'s energy budget. The MODIS BRDF/Albedo product provides an intrinsic characterization of surface anisotropy that is used to both determine global land surface albedos. The product relies on multi-date, clear-sky, atmospherically corrected surface reflectances coupled with a BRDF model to establish the surface anisotropy and provide albedo measures at a 500-m resolution in seven spectral bands and three broad bands. The surface anisotropy is also used to produce the nadir view-angle-corrected reflectances used by the MODIS land cover and phenology products.

B.10. MOD43B4: MODIS/Terra Nadir BRDF-Adjusted Reflectance 16-Day L3 Global 1 km

The MOD43B4 Nadir BRDF-Adjusted Reflectance (NBAR) Product (MODIS/Terra Nadir BRDF-Adjusted Reflectance 16-Day L3 Global 1 km SIN Grid) is computed for each of the MODIS spectral bands (1–7) at the mean solar zenith angle of each 16-day period. Since the view angle effects will have been removed from the directional reflectances, this will result in a more stable and consistent product. NBAR values are being directly used as the primary input to the advanced technique classifiers used in the production of the global MODIS Land Cover Product MOD12Q1. It is anticipated that the user community will be quick to take advantage of the NBAR data for those situations where composited surface reflectances may have been traditionally used.

In addition to the spectral NBAR values, the MOD43B4 NBAR Product also provides extensive quality information. Band-averaged quality information and band-independent data are stored in the first 32-bit word, while band-specific quality information and inversion status information are stored in the second 32-bit word. (Source: http://www-modis.bu.edu/brdf/userguide/nbar.html)